AN ABSTRACT OF THE THESIS OF

Rockie R. Yarwood for the degree of Doctor of Philosophy in Microbiology presented on August 20, 2001. Title: Interactions Between Microbial Dynamics, Water Flow, and Solute Transport in Unsaturated Porous Media.

Redacted for privacy

Abstract approved:_____

Peter J. Bottomley

Bioremediation in the vadose zone is unpredictable because of poor understanding of factors influencing microbial growth in this environment. A lab-scale experimental system was developed to examine, noninvasively, interactions between microbial growth, water flow, and solute transport in unsaturated porous media. Measurements of microbial colonization, and its impact on hydrology, were facilitated by using the *lux*CDABE-containing reporter bacterium *Pseudomonas fluorescens* HK44 and digital CCD imaging. Experiments were conducted in glass-walled two-dimensional flow cells (45 x 50 x 1 cm) packed with silica sand. Several bioengineering problems associated with chamber design and function required solution before microbial experiments were successful. These included: choice of materials for chamber components; development of sterilization, packing, and inoculation protocols; and development of procedures for data collection and chamber maintenance during experiments lasting several days. Bacterial growth was mapped daily by quantifying

development of salicylate-induced bioluminescence. A model relating the rate of increase in light emission after induction successfully predicted microbial densities over four orders of magnitude ($R^2 = 0.95$) provided that sufficient oxygen for the bioluminescence reaction was available. Total model-predicted growth during a one-week experiment agreed with potential growth calculated from the mass-balance of the system and previously established kinetic parameters (predicted, $1.2x10^{12}$ cells; calculated, $1.7x10^{12}$ cells). Although the rate of expansion of the colonized zone (and predicted populations in newly colonized regions) remained relatively constant, the proportion of the daily potential growth remaining within the chamber declined over time. Monitoring of bioluminescence revealed the development of an (hypothesized) anaerobic zone associated with microbial growth in the unsaturated porous media. Water content and flow streams were measured using light transmission. Accumulation of microbial growth modified the hydrologic properties of the sand causing up to 50% decrease in saturation within the colonized zone, diversion of flow around the colonized zone, and lowering (5 cm) of the capillary fringe height. Apparent solute velocity through the colonized region was reduced from 0.39 cm min^{-1} ($R^2 = 0.99$) to 0.25 cm min^{-1} ($R^2 = 0.99$). These experiments provide proof-of-concept for combining light transmission and bioluminescence technologies to study interactions between microbial growth and hydrology in unsaturated porous media.

INTERACTIONS BETWEEN MICROBIAL DYNAMICS, WATER FLOW, AND SOLUTE TRANSPORT IN UNSATURATED POROUS MEDIA

by

Rockie R. Yarwood

A THESIS

submitted to

Oregon State University

in partial fulfillment of
the requirements for the
degree of

Doctor of Philosophy

Presented August 20, 2001
Commencement June 2002

Doctor of Philosophy thesis of Rockie R. Yarwood presented on August 20, 2001.

APPROVED:

Redacted for privacy

Major Professor, representing Microbiology

Redacted for privacy

Chair of Department of Microbiology

Redacted for privacy

Dean of the Graduate School

I understand that my thesis will become part of the permanent collection of Oregon State University libraries. My signature below authorizes release of my thesis to any reader upon request.

Redacted for privacy

Rockie R. Yarwood, Author

ACKNOWLEDGEMENTS

I am grateful to my advisor Dr. Peter Bottomley, and to Dr. John Selker for their support and guidance over the course of my graduate studies. I also extend my appreciation to my other committee members, Dr. Daniel Arp and Dr. Jennifer Field, and to Dr. Linda Blythe. Special thanks to Dr. Larry Boersma for the crash-course in soil physics he provided during our visits to the coffee shop.

Many thanks go to my friends and co-workers on the project, Mark Rockhold, Mike Niemet, and Sandra Uesugi. I also would like to acknowledge Tulley Long, who assisted with some of the experimental assays.

To the many other friends I have made among the members of the Bottomley and Selker labs; Tom, Dave P., Khrys, Ieda, Lesley, Tracy, Aisha, Ann, Anne, Cham, Noam, Theresa, Thomas, Dave R., Jeff; I have enjoyed your companionship.

I thank the Department of Microbiology for providing a teaching assistantship and a grant from the N. L. Tartar foundation that funded my first two years of graduate study. Financial support for this work was provided by the National Science Foundation (grant #: 9630293) and the U. S. Department of Energy (grant #: DE-FG07-98ER14925).

Finally, words cannot adequately express my appreciation of my wife Jill, and daughters Anne and Sarah. Your constant love and encouragement, and your innumerable sacrifices, made this all possible. Thank you.

CONTRIBUTION OF AUTHORS

Dr. John Selker and Dr. Peter Bottomley were co-primary investigators on this project, and were involved in experimental planning and with editing of each manuscript. Mark Rockhold was involved with both experimental design and execution, and provided critical review of each manuscript. Mike Niemet provided valuable technical assistance with image analysis, assisted with experimental planning and construction of equipment, and provided critical review of each manuscript.

TABLE OF CONTENTS

TABLE OF CONTENTS (Continued)

LIST OF FIGURES

LIST OF TABLES

INTERACTIONS BETWEEN MICROBIAL DYNAMICS, WATER FLOW, AND SOLUTE TRANSPORT IN UNSATURATED POROUS MEDIA

CHAPTER 1

INTRODUCTION TO THE THESIS

MICROBIOLOGY IN THE SUBSURFACE ENVIRONMENT

The growth and transport of bacteria in subsurface environments is of considerable interest in a number of fields, including public health and environmental protection. Pathogenic bacteria and viruses in wastes disposed at the surface may contaminate groundwater. Many outbreaks of disease have been caused by contaminated groundwater (Craun, 1985). Microorganisms may significantly influence the fate and transport of contaminants in the vadose zone, either directly, by utilization of contaminants as metabolic or co-metabolic substrates, or indirectly, through microbial-induced modifications of their environment such as alterations in porosity, surface characteristics, pH, and redox (U. S. Dept. of Energy, 2000). The emergence of bioremediation as a viable technique for the restoration of contaminated soils and aquifers has led to increased interest in the understanding of bacterial behavior in the subsurface. Great potential lies in the ability to use bioremediation to degrade contaminants in place. However, at present, limited knowledge on the details of microbial growth in the subsurface hinders the further refinement of this technology.

Many researchers have studied microbiological and hydrological interactions in porous media under saturated flowing conditions (Oberdorfer and Peterson, 1985; Seki et al., 1998; Taylor and Jaffe, 1990; Vandevivere, 1995; Vandevivere and Baveye, 1992a, 1992b, 1992c; Wu et al., 1997). These studies reveal that saturated hydraulic conductivity is often reduced by several orders of magnitude as a result of growth and biomass accumulation over time. On the other

hand, studies addressing the impact of microbial growth on the hydrologic properties of unsaturated porous media are lacking (Rockhold et al., 2001; U. S. Dept. of Energy, 2000). Generally, studies of the relationships of microorganisms with hydrology in unsaturated media have focused either on the transport of organisms (Jewett et al., 1999; Powelson and Mills, 1996, 1998; Schafer et al., 1998; Tan et al., 1992, Wan et al., 1994), or on the biodegradation of model contaminants by bacteria (Allen-King et al., 1996; Estrella et al., 1993; Langner et al., 1998).

To overcome the present lack of understanding of the basic characteristics of microbial growth in unsaturated media and the resulting uncertainty in the prediction of biological degradation of contaminants in the vadose zone, it would be useful to be able to make real-time noninvasive measurements of microbial growth, water content distribution, and solute flow paths under unsaturated flowing conditions. Then, we could determine how water flow and solute transport spatially impact microbial growth, and, in turn, how microbial growth subsequently impacts water flow and solute transport. Recently, two noninvasive methodologies have emerged in the fields of subsurface hydrology and microbial ecology that are based on optical detection of light. These methodologies are the use of light transmission for measuring water content and solute transport in translucent porous media (Glass et al., 1989; Tidwell and Glass, 1994; Niemet and Selker, 2001), and the use of bioluminescent reporter systems for measuring microbial activity (Lindow, 1995; Stewart and Williams, 1992).

THE LIGHT TRANSMISSION METHOD

The light transmission method has been used for several years to study water behavior in unsaturated porous media. The method is based on the fact that the intensity of light transmitted through sand increases with increasing water content. Hoa (1981) took advantage of this observation, and developed the light transmission method for determining water content in thin slabs of porous media. Hoa used a point source of light and a detector to measure water content at discrete locations in the sand. Glass et al. (1989), and Tidwell and Glass (1994) improved the method by introducing the use of two-dimensional glass-walled flow cells back-lit by banks of fluorescent lights and imaged with video cameras. Digitization of the images allowed obtaining hundreds-of-thousands of discrete measurements in the time it took to obtain one measurement with Hoa's device. The recent advent of the use of CCD cameras has provided additional improvement because they are very sensitive to low levels of light. Furthermore, there is a precise linear relationship between the light intensity and the recorded data, and the image is already digitized, ready for analysis. Selker (1991) extended the light transmission method to make observations of solute distribution by using applications of dyed solutes and time-lapse video recording. Schroth et al. (1995, 1998) applied the method to study nonaqueous-phase liquid movement in water-wetted porous media. Niemet and Selker (2001) made significant refinements in both the precision and the ease of water content measurement with light transmission. Their method was

the first to overcome the necessity to calibrate a particular system and media against another technique, such as x-ray or gamma-ray transmission.

BIOLUMINESCENT REPORTER ORGANISMS

Bacterial *lux* gene-dependent bioluminescence has become a useful tool for microbial ecologists. Bacterial luminescent systems contain genes encoding the α and β subunits of the luciferase enzyme (*luxA* and *luxB*) and genes encoding the reductase, transferase, and synthetase components (*luxC*, *luxD*, and *luxE* respectively) of a fatty-acid reductase enzyme complex (Meighen, 1988, 1991, 1993). The bacterial luciferase enzyme catalyzes the oxidation of reduced flavin mononucleotide ($FMNH_2$) and a long-chain fatty aldehyde with the resultant emission of blue-green light at a wavelength of 490 nm.

$$FMNH_2 + O_2 + RCHO \rightarrow RCOOH + FMN + H_2O + \text{light (490 nm)}$$

The level of light generated *in vivo* by the reaction is thus dependent on the availability of oxygen from the environment, and on levels of intracellular pools of reducing equivalents and fatty-acids that are in turn dependent on the metabolic state of the cell. The fatty-acid reductase is responsible for the sequestration of cellular fatty acids into the fatty-acid reductase reaction, and for recycling of the oxidized product of the light emitting reaction to aldehyde thus replenishing one of the reaction substrates. Figure 1.1 briefly outlines the reactions involved in bacterial bioluminescence. The physiological, biochemical and genetic aspects of

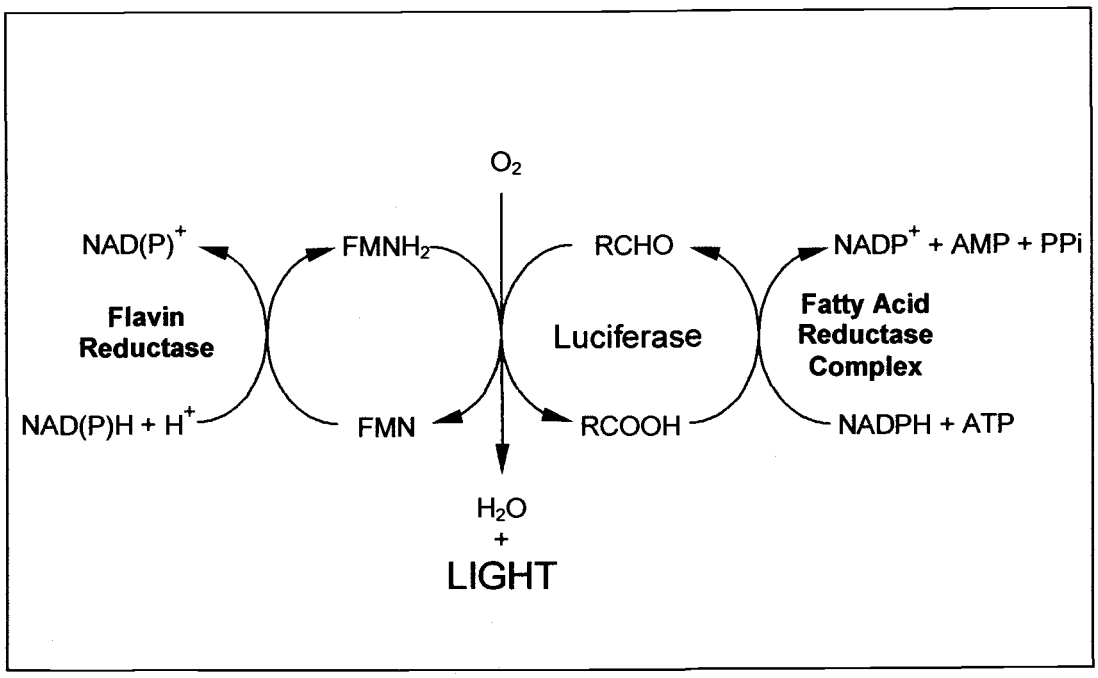

Figure 1.1. The reactions of bacterial bioluminescence.

bacterial bioluminescence have been exhaustively examined, and a number of excellent reviews have been published (e.g. Hastings and Nealson, 1977; Meighen, 1988, 1991, 1993; Meighen and Dunlap, 1993; Stewart, 1990; Stewart and Williams, 1992; Tu and Mager, 1995; Wilson and Hastings, 1998).

In recent years, bacterial lux genes have been used to detect and to monitor the fate of microorganisms introduced into natural environments (deWeger et al., 1991; Flemming et al., 1994a, 1994b; Rattray et al., 1990; Shaw et al., 1992), and to study the interactions of bacteria with plants (Beauchamp et al., 1993; Shaw and Kado, 1986; Shaw et al., 1987; Waterhouse et al., 1996; Yeomans et al., 1999). They have also been used as an indicator of bacterial metabolic state (Duncan et al., 1994; Meikle et al., 1992), and as indicators of the presence of toxicants such as antibiotics (Soren et al., 1995). In addition, *lux* gene fusions to inducible catabolic genes of environmental importance have been used to detect bioavailable concentrations of organic contaminants and heavy metals in the environment (Applegate et al., 1998; Blouin et al., 1996; Burlage et al., 1990; King et al., 1990; Heitzer et al., 1992, 1994; Selifonova et al., 1993; Sticher et al., 1997). Recent studies have reported on the use of *lux*-marked strains to study bacterial activity in saturated flow columns (Neilson et al., 1999; Yolcubal et al., 2000).

By combining the two light-based technologies described above, light transmission chambers and bioluminescence, it might be possible to develop a useful tool to study the interactions of microbial growth, water flow and solute transport in unsaturated porous media. Use of a bioluminescent bacterium to

colonize the media within the chamber might allow for the monitoring of the spatial and temporal development of microbial growth by imaging the bioluminescence with a CCD camera. Water content and solute flow paths could be monitored with the light transmission method, also imaging with the CCD camera. At the time these studies were initiated, no one had evaluated whether the current design of light transmission chambers was adequate for incorporating a microbiological component, or whether it would be feasible to quantify microorganisms by bioluminescence in such a system.

The bacterium selected for this work is the bioluminescent reporter strain *Pseudomonas fluorescens* HK44, developed by Professor Gary Sayler's group at the University of Tennessee, Knoxville, TN (King et al., 1990). *P. fluorescens* HK44 carries a *nahG-luxCDABE* transcriptional fusion in the lower pathway of the naphthalene degradation plasmid pUTK1. Plasmid pUTK1 bears homology to the classical NAH7 naphthalene degradation plasmid that has been extensively characterized in the literature (see for example Yen and Gunsalas, 1985; Yen and Serdar, 1988; Schell, 1990). Exposure of *P fluorescens* HK44 to naphthalene or its metabolite, salicylate, results in the emission of measurable quantities of light from the *lux* system. *P. fluorescens* HK44 has been extensively characterized for the specificity and kinetics of its bioluminescent response upon exposure to naphthalene, salicylate, and other chemicals, and for its utility as a biosensor for detection and quantification of bioavailable hydrocarbon

contaminants in environmental samples (King et al., 1990; Heitzer et al., 1992, 1994, 1998; Matrubutham et al., 1997; Webb et al., 1997).

Parallel studies conducted in our laboratory demonstrated the ability to utilize the bioluminescence of *P. fluorescens* HK44 in response to salicylate to quantify population density in liquid culture and in saturated and unsaturated sands under static conditions (Uesugi et al., in review) and resulted in development of a model describing the cell-density-dependent bioluminescence response of *P. fluorescens* HK44. In the model, it is the rate of increase in the rate of light production after exposure to the inducer, rather than an absolute light level, that is related to cell density. For cells in the presence of sand, the model is expressed in the equation:

$$(L/c)^{1/2} = tn\phi(\theta)(B'/2)^{1/2}$$

where L is light units per minute (LUPM) (CCD counts divided by the exposure time in minutes), c is the *P. fluorescens* HK44 cell density in CFU mL^{-1} of pore liquid, t is the time in minutes since exposure to salicylate, and B' is the rate of increase in cellular light production rate with units of (LU / [cell-min^2]). The terms n and $\phi(\theta)$ account for the attenuation of detected light emission from sand where n is the porosity and $\phi(\theta)$ describes the effect of water content. The $\phi(\theta)$ relationship was determined empirically.

There are several significant differences between the experimental system used by Uesugi et al. (in review) and the 2D flow cell system. For example, Uesugi's experiments were carried out in batch reactors with non-growing cells

under non-flowing conditions, and the induction time, t, since exposure to salicylate was constant for the entire imaged area. The volumetric water content, θ, used to obtain $\phi(\theta)$, was constant, the entire volume was uniformly colonized with a single cell density, and salicylate was present for the duration of the experiment.

Under conditions of unsaturated flow in the dynamic experimental system proposed here, water content and cell density would both vary with position in the chamber. Furthermore, the time of first exposure to salicylate would vary with both position and with water content. Microorganisms within the experimental domain probably would be in various stages of growth. Salicylate would be applied intermittently for a limited duration, and oxygen for the light reaction would be replenished continuously by flowing media.

OBJECTIVES

Given the strong interest in and limited knowledge about microbiology in the vadose zone, coupled with the challenge of marrying the two light-based technologies for microbial-hydrology studies, the overall goal of my thesis became focused on examining the possibility that light transmission chambers could be adapted for studying microbiological behavior under unsaturated flowing conditions.

Specific objectives were:

1. To adapt the 2D light transmission chambers for successfully carrying out microbiological experiments (Chapter 2).

2. To determine if the Uesugi model would successfully quantify *P. fluorescens* HK44 growing under unsaturated flowing conditions in the 2D chambers (Chapter 3).
3. To noninvasively map the spatial and temporal development of microbial colonization in the 2D chambers under unsaturated flowing conditions (Chapter 3).
4. To noninvasively monitor the impact of microbial colonization on the hydrologic properties of the porous medium using light transmission technology to measure water contents and solute flow paths (Chapter 4).

CHAPTER 2

A NOVEL EXPERIMENTAL SYSTEM FOR NONDESTRUCTIVE MONITORING OF INTERACTIONS BETWEEN MICROBIAL GROWTH, WATER FLOW, AND SOLUTE TRANSPORT IN UNSATURATED POROUS MEDIA

R. R. Yarwood[1], M. L. Rockhold[2], M. R. Niemet[2], J. S. Selker[2], and P. J Bottomley[1]
[1]*Department of Microbiology and* [2]*Department of Bioengineering,*
Oregon State University, Corvallis, OR 97331, USA

ABSTRACT

A novel experimental system was developed that permits noninvasive observation of microbial distribution and activity, as well as water content and solute transport in unsaturated porous media. The system consists of a 45 x 56 x 1 cm two-dimensional flow cell with glass sheets confining a thin slab of siliceous porous medium. Induction of bioluminescence provides for the observation of the spatial and temporal development of colonization, and light transmission provides for simultaneous measurement of water contents and flow paths in the system. Digital CCD imaging is used to nondestructively monitor the system over time and provides an outstanding density of information at high spatial resolution. Comparisons were made of light transmission through colonized and uncolonized sands to determine whether the presence of microorganisms would significantly attenuate transmitted light. The average value for the ratio of transmitted light in the presence of 10^9 CFU mL^{-1} to transmitted light in the absence of cells was 1.001 (SD 0.003) under unsaturated conditions and 0.994 (SD 0.006) under saturated conditions. Water contents determined by the light transmission method were in close agreement with those determined by the gravimetric method upon destructive sampling of colonized sand despite cell densities approaching 10^{11} CFU mL^{-1} of pore water. A description of the system and methodology is given together with illustrative examples of collected imagery.

INTRODUCTION

Protection of groundwater resources from contamination by chemicals applied or spilled at the surface is of major importance. Great potential lies in the ability to use bioremediation to degrade contaminants that have entered soils in place. However, at present our knowledge is limited about the details of microbial growth under conditions of unsaturated flow in the vadose zone. Real-time measurements of microbial activities and growth responses in unsaturated porous media are needed to determine how water flow and nutrient transport features spatially impact microbial growth, and in turn, how that microbial colonization subsequently impacts water flow and solute transport. This work was directed toward the development and utilization of a novel method to examine these interactions. The method brings together two recently developed optical technologies: the use of light transmission systems to quantify pore water content and flow paths; and the use of bioluminescent bacteria to measure microbial activity.

The light transmission method

The intensity of light transmitted through translucent porous media increases with increasing water content. Hoa (1981) applied this observation by developing a device to measure the degree of water saturation at a point within a thin slab of sand. Glass et al., (1989) and Tidwell and Glass (1994) advanced the method by using banks of fluorescent bulbs to backlight thin slabs of sand packed

between pairs of parallel glass sheets (2-D chambers), and using video cameras to image light transmitted through the entire chamber simultaneously. Selker (1991) utilized the method to observe solute distribution over long periods of time by application of dyed solutes and time-lapse video recording. Schroth et al. (1995, 1998) applied the method to study nonaqueous-phase liquid movement in water-wetted porous media. Recently, digital CCD imaging has been used to improve data quantification, and Niemet and Selker (2001) made significant refinements in the precision of quantifying water content in quartz sands by this method.

Bacterial bioluminescence

Bacterial *lux* gene-dependent bioluminescence has become an important tool for microbial ecologists. Bioluminescence has been used to monitor the fate of microorganisms introduced into natural environments (Shaw et al., 1992; Rattray et al., 1990; Flemming et al., 1994a, 1994b; deWeger et al., 1991), to study plant-microbe interactions (Shaw and Kado, 1986; Shaw et al., 1987; O'Kane et al., 1988; Beauchamp et al., 1993; Bolenes et al., 1993; Yeomans et al., 1999), and has also been used as an indicator of bacterial metabolic state (Duncan et al., 1994; Meikle et al., 1992). In addition, *lux* gene fusions to inducible catabolic genes have been used to detect bioavailable concentrations of organic contaminants and heavy metals in the environment (Applegate et al., 1998; Burlage et al., 1990; King et al., 1990; Heitzer et al., 1992, 1994; Blouin et al., 1996; Selifonova et al., 1993, Sticher et al., 1997). Recent studies have reported on the use of *lux*-marked strains to study

bacterial activity in porous media under saturated flowing conditions in columns equipped with fiber-optic probes (Neilson et al., 1999; Yolcubal et al., 2000).

In this paper, we describe our efforts to adapt the 2-D light transmission chambers to study the interactions of a *lux*-gene-containing bacterium with the hydrologic components of a porous medium under unsaturated flowing conditions. Our system permits direct, continuous observation of microbial distribution and activity, as well as water content and solute transport in unsaturated porous media. A description of the system and methodology is given in the following together with illustrative examples of collected imagery.

SYSTEM DESCRIPTION AND METHODS

Chamber and associated equipment

The light transmission chamber and associated equipment used in this work are shown in Figures 2.1, 2.2, and 2.3. The chamber consists of two, 51.0 cm wide by 61.0 cm high by 1.3 cm thick plate glass sheets separated by a 1.0 cm thick U-shaped aluminum spacer (Fig. 2.1a). The glass sheets are sealed to the spacer by fluorocarbon rubber o-ring stock (Viton®, Dupont Dow Elastomers, Wilmington, DE) inset into groves machined into each face of the spacer. The lower side of the spacer has been machined with a drain port and an integral manifold surmounted with a 10 μm nominal (16-18 μm absolute, giving an air-entry pressure of about 165 cm H_2O) pore-size Twilled Dutch Weave stainless steel wire screen (Screen Technology Group, Inc., Washougal, WA). The use of this fine-mesh screen

Figure 2.1. Two-dimensional flow chamber. 2.1a: sectional views through the porous medium-containing portion of the chamber, the influent manifold, and UV unit. Key: A, germicidal lamp; B, influent drip emitters; C, siphon tube; D, glass sheets; E, spacer; F, o-ring seal; G, micro-porous screen; H, effluent manifold; I, drain port. 2.1b: assembled chamber unit mounted to the light box. Key: A, ballasts for light bank; B, fluorescent tubes; C, chamber; D, chamber frame; E, clamp adjustment screws; F, cooling fan.

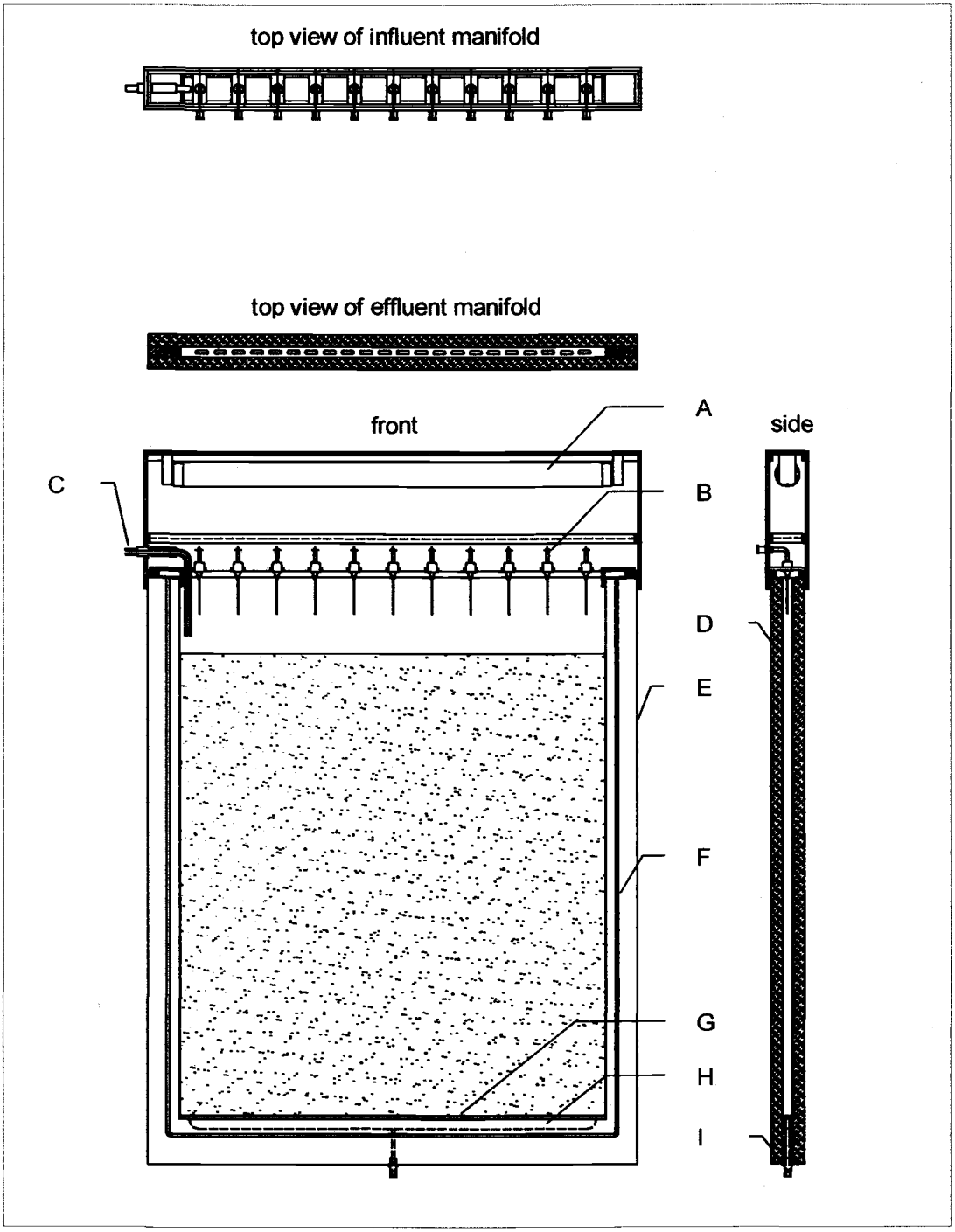
top view of influent manifold
top view of effluent manifold
front
side
A
B
C
D
E
F
G
H
I

Figure 2.1a.

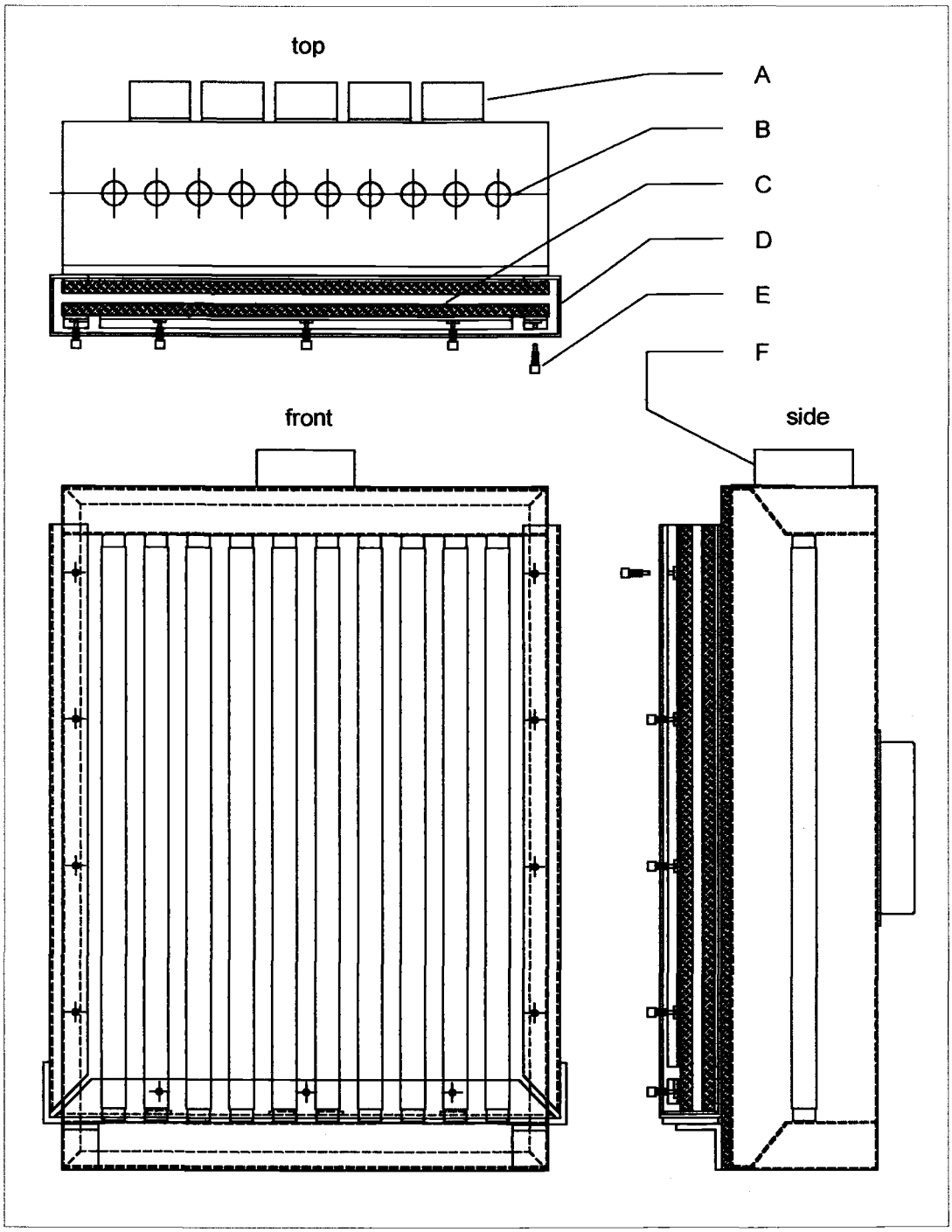

Figure 2.1b.

allows adjustment of the relative proportions of unsaturated and saturated media within the chamber by raising or lowering the elevation of the effluent outlet. The elevation of the open end of the effluent tube is set to obtain the desired boundary pressure, which in turn controls the height of the capillary fringe within the chamber. The chamber is held together by clamping within an aluminum frame (Fig. 2.1b). When assembled, the internal chamber dimensions are 44.5 cm wide by 56.0 cm high by 1.0 cm thick. The glass sheets can be drilled with various configurations of ports to allow inoculation or sampling of the chamber. The ports are sealed with high temperature silicon sealer to allow injection or sampling via syringe. All chamber materials were selected to be resistant to autoclaving. The chamber is filled via a stainless steel prismatic funnel (not shown) that contains three coarse screens to randomize the trajectories of the falling sand particles. A 4 kg capacity hopper is built onto the upper portion of the funnel to hold the sand. A stainless steel sliding gate opens or closes the hopper drain openings as needed.

The chamber assembly mounts to a fan-ventilated sheet metal housing containing a light bank of 10 fluorescent tubes (Philips F17T8/TL835, 61 cm) (Fig. 2.1b). The light bank provides the source of illumination for light transmission images. The entire chamber/light box unit attaches to a sturdy mount that can be rotated to a horizontal position to facilitate easy sampling of the chamber contents at the conclusion of an experiment (Fig. 2.2).

The fluid application system (influent manifold) (Fig. 2.1a) uses syringe-needle drip-emitters, the number and spacing of which can be varied to suit

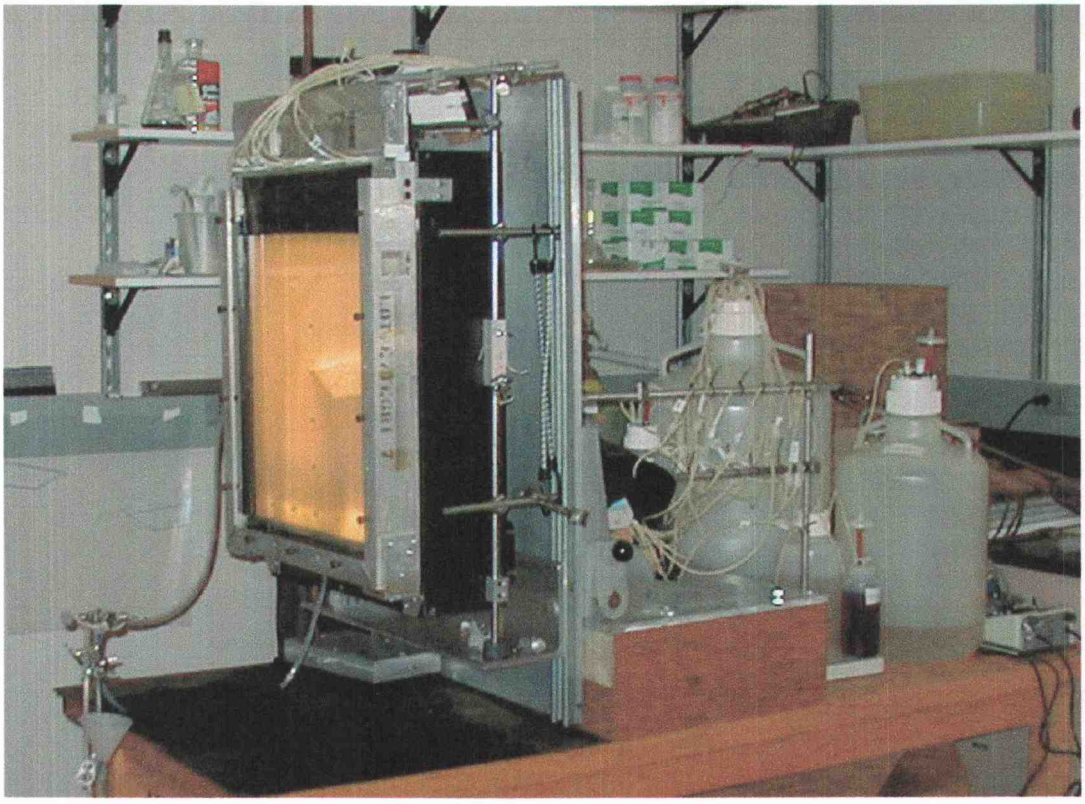

Figure 2.2. Photograph of assembled chamber and rotating mount.

experimental requirements. For the experiments illustrated here, eleven, 23-guage emitters were spaced 4.1 cm apart. Feed lines connect via individual fittings in the front face of the housing. Each emitter is fed individually via a multichannel peristaltic pump. This strategy allows precise control of the flow rate through each emitter and eliminates the problem of periodic stoppages that may occur when multiple emitters are fed via a common reservoir. The housing also contains a glass siphon tube that allows liquid to be removed from the chamber when upward flow is used, such as when the chamber is initially saturated. Free exchange of air to the upper chamber is facilitated by the addition of several ports equipped with 0.2-micron inline filters.

The upper portion of the housing contains a 15-watt germicidal lamp (G15T8, General Electric, Cleveland, OH) that is used to irradiate the drip emitters and the surface of the sand with UV-C light. In earlier work we encountered a recurring problem of contamination of the influent solutions due to aerosolized bacteria from within the chamber that came in contact with the needles. Addition of a germicidal lamp unit completely eliminated the problem. The positioning of the lamp provides a dose of greater than 100,000 $\mu W\ cm^{-2}$ to the surface of the sand during a 60 s exposure. The lamp is operated periodically throughout the course of an experiment by use of a computer-controlled timer.

Feed solutions are held in autoclaveable carboys (Nalgene, Rochester, NY) with ventilated closures equipped with 0.2-micron filters. Solutions are supplied to the chamber via multichannel peristaltic pumps (Cole-Parmer, Vernon Hills, IL).

Light detection system

The light detection system (Fig. 2.3) currently in use consists of a liquid-cooled 16-bit digital camera with a backlit SITe model SI-502A 512 x 512 pixel scientific grade CCD array and ST-138 controller (Princeton Instruments, Inc., Trenton, NJ). The CCD chip is cooled to -50°C to minimize the dark charge effect (thermally generated electrons within the silicon) inherent in CCD devices and improve the signal to noise ratio. The camera lens used currently is a Nikon 50 mm, f-1.8 (Nikon Corporation, Tokyo, Japan). Light transmission images are obtained using a 620 nm center-wavelength, 10 nm bandpass filter (Oriel model # 59410, Oriel Co., Stratford, CT) placed in front of the lens. Bioluminescence emission images are made without filtration. The distance from the chamber to the lens is 1.9 m. With this system geometry, each image pixel represents approximately 1 mm^2 of chamber surface area. Each image provides more than 200,000 discrete measurements over the experimental domain.

Porous medium

The porous medium used in this work is optically translucent silica sand sold under the trade name Accusand® (Unimin Corp., LeSueur, MN). The physical, chemical, and optical properties of this material have been well characterized (Schroth et al., 1996; Niemet and Selker, 2001). Sand is prepared by soaking in 5 M NaCl followed by a thorough rinsing with deionized water. This treatment removes fine particulates. The washed sand is then portioned into wide-mouth Kimax® (Kimble, Vineland, NJ) 2.8 L Fernbach flasks loosely sealed

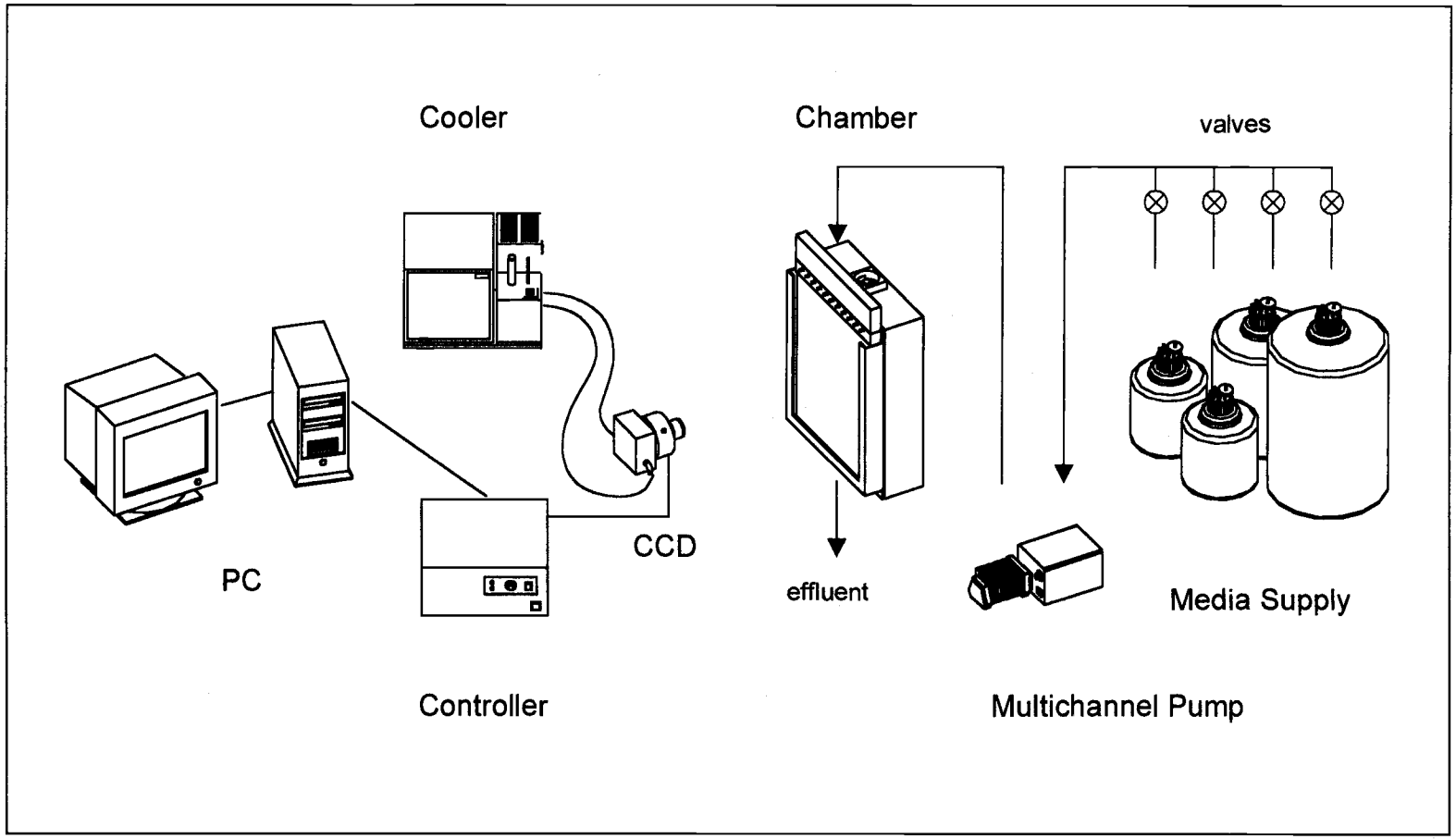

Figure 2.3. Diagram of experimental system components.

with cotton plugs and aluminum foil covers. The damp sand is autoclaved three times for one hour each time, and allowed to stand at room temperature for at least 24 hours between each sterilization. Preliminary experiments revealed that at least two rounds of autoclaving were required to insure sterility of the sand. After autoclaving for the third time, the sand is oven dried to constant weight at 50°C.

Bacterial strain, media, and growth conditions

Pseudomonas fluorescens HK44 was kindly supplied by Gary Sayler, University of Tennessee, Knoxville, TN. *P. fluorescens* HK44 harbors the plasmid pUTK21 containing the *luxCDABE* gene cassette and a tetracycline resistance marker (King et al., 1990) and has been extensively characterized for the specificity and kinetics of its bioluminescent response upon exposure to naphthalene, salicylate, and other chemicals, and for its utility as a biosensor for detection and quantification of bioavailable hydrocarbon contaminants in environmental samples (Heitzer et al., 1992, 1994, 1998; King et al., 1990; Matrubutham et al., 1997; Uesugi et al., 2001; Webb et al., 1997). Exposure of this bacterium to naphthalene or salicylate results in light emission at 490 nm from the *lux* system. All media are supplemented with 15 mg L^{-1} tetracycline (Tet15). The strain is stored at -80°C in 20% glycerol. Working stocks are maintained on plates containing half-strength TSB (Difco Laboratories, Detroit, MI) supplemented with 15 mg L^{-1} tetracycline and 1.5% Bacto Agar. The liquid medium used in the experiments described here is a modified minimal mineral salts (MMS) containing the following (in grams per

liter): $CaCl_2 \bullet 2H_2O$, 0.05; $(NH_4)_2HPO_4$, 1.2; KH_2PO_4, 5.6; $MgSO_4 \bullet 7H_2O$, 0.2; $Na_2EDTA \bullet 2H_2O$, 0.0099; $FeCl_3$, 0.004; HCl, 0.00365; H_3BO_3 0.00143; $MnSO_4 \bullet 4H_2O$, 0.00102; $ZnSO_4 \bullet 2H_2O$, 0.00022; $CuSO_4 \bullet 5H_2O$, 0.00008; $CoCl_2 \bullet 4H_2O$, 0.0001; $Na_2MoO_4 \bullet 2H_2O$, 0.00005. The pH is adjusted to 7.0 with a concentrated solution of KOH (about 1.44 g KOH L^{-1} MMS). Glucose, at 250 mg L^{-1}, (Glu250) served as carbon source in all the experiments illustrated here. A saturating concentration of the *lux* inducer salicylate (100 mg L^{-1}; Sal100) was used to induce the bioluminescent response. Glucose, salicylate, and tetracycline were obtained from Sigma Chemical Co., St. Louis, MO.

Preparation of equipment

Before assembly, the glass panels are cleaned consecutively with ammonia-based window cleaner and acetone. The spacer is washed with LpH® germicidal detergent (Calgon, St Louis, MS) and thoroughly rinsed with hot water. After assembly, the chamber is sterilized by autoclaving and allowed to dry for several days. In initial experiments, we attempted to sanitize the chamber assembly with a bleach solution prior to packing with sand, but found that treatment inadequate to completely eliminate contamination. Over the course of the one-to-two week-long experiments, growth of contaminants would occur despite the presence of tetracycline. We also attempted additional sterilization steps after chamber packing, such as flooding the packed chamber with a solution of 70% ethanol, or with a mixture of several antibiotics. These additional treatments were

only partially successful, allowing experiments to remain free from significant contamination for only one-to-two days longer than before. Furthermore, the ethanol treatment caused undesirable changes in the hydraulic properties of the sand. Attempts to autoclave the chamber assembly after packing with sand were not successful, because differential expansion of the chamber materials during autoclaving allowed the packed sand to slump.

The influent manifold housing is washed with germicidal detergent, rinsed with hot water, and allowed to dry. The drip emitter fittings and tubing are autoclaved, and assembled under a laminar flow hood. After assembly, all surfaces of the unit are sterilized by ultraviolet light, and the unit is wrapped in sterilized aluminum foil. Each carboy and all tubing is thoroughly washed and then autoclaved. The funnel/hopper assembly is washed, autoclaved, and then allowed to dry.

Chamber packing

Chamber packing is carried out under a modified laminar flow hood, with its sides and top extended in order to accommodate the chamber and hopper assemblies. First, sufficient sand is added to the hopper to fill the entire chamber with excess. A line marked on the front glass sheet of the chamber at a desired distance above the surface of the effluent manifold screen serves as a guide for filling the chamber. The loaded funnel/hopper assembly is weighed, then placed on top of the chamber, and the gate opened to release sand from the hopper. The fill is stopped shortly after the packing front has passed the fill line. The overburden is

removed by vacuuming through a sterile tube. The vacuum unit is kept sufficiently far from the chamber to avoid disruption of the laminar flow air within the hood. The funnel assembly plus remaining sand, and the sand removed by vacuum are weighed, and the mass of sand in the chamber calculated by difference. Immediately after the overburden is removed, the upper interior of the chamber and sand surface is irradiated with UV light for one minute.

Influent flow rate calibration and initial chamber saturation

After all tubing connections are made, trapped air is removed by pumping the media solutions through the tubing. Sterile syringe needles are attached and the drip emitters are calibrated by pumping the liquid into preweighed beakers. The entire process is carried out under constant UV irradiation to maintain sterility. After the drippers are calibrated, flow is stopped and the influent manifold and UV unit are attached to the chamber. At this time, the chamber assembly is attached to the light box.

Prior to saturation, the chamber is slowly purged through the lower port with 0.2 micron-filtered CO_2 gas to displace all of the air within the pore space of the sand (the flow rate must be kept low to avoid disturbing the sand pack). This treatment minimizes the risk of entrapped air when the chamber is first filled with liquid, because CO_2 is more soluble than air. Sterile MMS is delivered slowly through the lower port and the chamber allowed to fill until ponding occurs. The siphon tube in the influent manifold is then opened and several pore volumes of MMS are pumped through the system from the bottom up and siphoned off to

waste. This insures that all traces of CO_2 are removed from the system. Several portions of the overflow are collected and later assayed for microbial contamination by inoculating into nutrient broth and incubating for several days. After flow is stopped, a light transmission image is made of the saturated chamber. Prior to inoculation, dark images (see explanation in image analysis section) are obtained.

Preparation of cells and inoculation

P. fluorescens HK44 is grown overnight in MMS+Tet15 supplemented with 1.0 g L^{-1} glucose at 27°C with shaking at 150 rpm. The culture is centrifuged, washed with MMS basal medium, and resuspended to the desired density in MMS. Inoculation is generally made by injecting a volume of cell suspension through a port in the front sheet of the chamber directly into the saturated sand at the desired depth below the surface. In early experiments, the sand was colonized uniformly by adding the cells along with the medium used to saturate the sand. Invariably, this resulted in the majority of growth occurring at the upper sand surface, where substrate and oxygen were most plentiful, rather than within the interior of the sand pack. The inoculated, saturated chamber is allowed to stand for one hour, whereupon the effluent port is opened to allow the chamber to drain. Once the water content reaches steady state, a transmission image of the unsaturated condition is obtained, and influent flow is started.

Data collection

Liquid saturation. Transmission images are made to determine water

content distribution. The CCD and chamber light bank are turned on and allowed to come to temperature equilibrium, and, with the room lights off, 0.08 s exposures are obtained at an aperture setting of f-1.8 and with the 620 nm-centered 10 nm-bandpass filter. Filtration simplifies the use of light transmission for measuring water content and flow paths in our system because the light source emits a continuum of wavelengths and the media used in our experiments are not colorless. The intensity of light transmitted through a medium (I) depends on the intensity of the source (I_0), the absorption coefficient of the medium (α), and the thickness of the medium (d) as described by Beer-Lambert's law:

$$I = I_0^{(-\alpha d)} \qquad (1)$$

where α depends on both the color of the media and the wavelength of incident light.

Flow paths. Flow paths are determined using an application of bromophenol blue dye. A concentration in the range of 0.001% (w/v) to 0.01% (w/v) was found suitable for detection. Concentrations of 0.0001% or 0.1% were too low or too high, respectively, to clearly discern variations in light attenuation within the plume. Batch experiments revealed that the dye was not toxic to *P. fluorescens* HK44 at the concentrations used and did not sorb to cells or to sand. The progress of the dye plume through the chamber is recorded with a series of transmission images at timed intervals. The exposure times, aperture and filtration are the same as for the liquid saturation images.

Bioluminescence. The influent drip emitters are switched to a solution of

MMS+Tet15+Sal100, except for the glucose application dripper (or drippers, depending on the experiment), which is switched to a solution of MMS+Tet15+Glu250+Sal100. Salicylate is applied onto the chamber for 150 min, after which the feed system is restored to the standard solutions. The light response is recorded in a series of 10 min exposures at 20-minute intervals with an aperture setting of f-1.8 and without filtration. Any colored filter placed in the light path will decrease the intensity of light that reaches the CCD. Moreover, the majority of the light from bioluminescence is emitted at wavelengths near 490 nm. Light emitted in the bioluminescence reaction is of very low intensity and requires exposure times of several minutes with our system. Filtration would require the use of even longer exposure times.

Image analysis

The signal to noise ratio in a CCD image is degraded by signal contributions from the analog/digital converter (bias signal), thermally generated electrons within the semiconductor (dark charge), and background ambient light. Cooling of the CCD helps to minimize the dark charge. Background ambient light levels are minimized by darkening the room that houses the chamber and camera. All sources of stray light within the room are masked (indicator lamps on power supplies, pumps, and computer equipment), and openings in walls, ceiling, and around vents and the doorway are masked to reduce stray light leaking in from outside the room. In order to remove these effects from the raw CCD data, images of equal exposure time and f-stop for both transmission and emission images are

made prior to the start of each experiment with the light bank off (dark images) and subtracted from each data image. After dark image subtraction, the following additional steps are carried out.

The absolute water saturation, S, is determined for all points within the sand-filled region of the chamber by the method of Niemet and Selker (2001), where for 40/50 Accusand

$$S = \left[0.19\Omega^4 - 0.24\Omega^3 + 0.19\Omega^2 - 1.14\Omega + 1\right](1 - 0.057) + 0.057 \qquad (2)$$

and

$$\Omega = \ln\left(\frac{I}{I_s}\right) \Big/ \ln(0.07) \qquad (3)$$

I represents the image of interest and I_s represents the saturated image. The volume of water resident within a region of pixels is computed as follows

$$V = \sum SV_{pix}n \qquad (4)$$

where V_{pix} is the bulk volume of chamber space occupied by a pixel and n is the porosity.

For determination of flow paths, the relative attenuation of transmitted light due to the dye is obtained by taking the ratio of a transmission image made immediately prior to the start of the dye pulse over each of the transmission images obtained during the pulse. A comparison of sums of all data points within each image, for a series of images in which the entire dye pulse was contained within the imaged region of the chamber, revealed that conservation of mass was maintained, indicating that relative attenuation of transmitted light in our system is a good

surrogate for a measure of dye concentration (data not shown). If desired, quantification of dye plume concentration may be achieved empirically from the following equation based on Beer's law:

$$C/C_0 = \left[\frac{-\ln\left(I_{dye}/I_{dye,0}\right)}{xS^y}\right]^z \quad (5)$$

where x, y, and z are empirical constants determined from a second calibration experiment, and S is the liquid saturation determined using equation (2).

Because image processing involves combining pixel-by-pixel data obtained at different times, both the CCD and the chamber must be rigidly mounted to maintain precise alignment throughout the course of an experiment. Image processing was performed using Transform 3.4 (Fortner Software LLC, Sterling, VA).

Experiments

Impact of cell suspensions on apparent saturation as determined by light transmission. A light-transmission chamber was packed with 40/50 mesh sand and the lower zero-pressure boundary was set at about one cm above the lower edge of the sand pack. Under these conditions the capillary fringe rose to slightly below the vertical midpoint of the sand pack. The upper half remained unsaturated at a volumetric water content of about 0.12 $cm^3\ cm^{-3}$. MMS medium was applied to the surface of the sand through eleven equally spaced drip emitters at a total flow rate of 315 mL h^{-1}. After allowing the system to reach equilibrium, a series of light transmission images was made. Next, the five rightmost drip emitters were

switched to a solution of MMS containing *P. fluorescens* HK44 at 1×10^8 CFU mL^{-1} and the five leftmost drippers were switched to a solution of MMS containing *P. fluorescens* HK44 at 1×10^9 CFU mL^{-1}. Application of MMS alone was continued from the central dripper to provide a buffer strip that prevented mixing of the two cell solutions. Transmission images were then obtained at five-minute intervals over a three-hour period while the cell solutions moved through the system. Image analysis was carried out over four regions (76 by 76 pixels) that each represented one of the experimental conditions (1×10^8 CFU mL^{-1}, unsaturated; 1×10^8 CFU mL^{-1}, saturated; 1×10^9 CFU mL^{-1}, unsaturated; 1×10^9 CFU mL^{-1}, saturated).

Example homogeneous texture experiments. A light-transmission chamber was packed with 40/50-mesh sand. The effluent outlet was positioned 0.5 cm above the lower boundary of the sand. As described above, this resulted in saturation of the lower half sand pack while the upper half of the sand pack remained unsaturated. A 5 mL aliquot (5×10^8 CFU mL^{-1}) of a *P. fluorescens* HK44 suspension was inoculated through a sampling port at a depth of 15 cm below the sand surface. MMS medium was applied to the surface of the sand through 11 equally spaced drip emitters at a total flow rate of 316 mL h^{-1}. Glucose (250 mg L^{-1}) was supplied continuously through the center dripper only. Light transmission images for water-saturation were obtained several times each day. Bioluminescence was induced daily by the addition of salicylate through all drippers, and monitored with the CCD camera. Emission intensity is presented in

arbitrary light units. Flow paths were monitored daily by addition of a 0.01% (w/v) bromophenol blue dye solution to the center dripper. Switching of solutions was accomplished without interrupting flow.

Comparison of water content determination by light transmission and gravimetric analysis. At the conclusion of the homogeneous texture experiments described above, the chamber contents were destructively sampled and water content distribution was determined gravimetrically. A sampling grid was drawn on a clear Mylar sheet that was attached to the chamber front glass. A CCD image was taken to provide a reference between image data and sampling data. The glass-sand-glass sandwich was then removed from the frame and placed face down with the upper end slightly elevated. The rear sheet of glass was carefully removed and the exposed sand was covered with plastic film to retard drying. Samples of the sand (2.5 cm x 2.5 cm x 1.0 cm) were collected according to the grid pattern that was visible through the front glass sheet, while exposing only a small portion of the sand at a time. The *Pseudomonas fluorescens* HK44 population density was quantified by dilution plating of sand samples on half-strength TSB (tryptic soy broth) agar amended with tetracycline. For gravimetric analysis, sand samples were added to preweighed microfuge tubes. The total wet weight of the tube and moist sand was obtained; then the samples were oven dried at 50°C to constant weight and the difference determined. Results were compared with water content measurements determined using the transmission method immediately prior to destructive sampling.

RESULTS AND DISCUSSION

Experiments

Impact of cell suspensions on apparent saturation as determined by light transmission. A commonly used method for estimating bacterial cell density in liquid suspensions is based on spectrophotometric measurement of turbidity. The level of light-scattering, expressed as absorbance, increases in proportion to the density of cells present in the solution. Therefore it was important to determine if bacterial cell suspensions would influence apparent saturation determined by light transmission (Fig. 2.4). The average value for the ratio of transmitted light in the presence of 10^9 CFU mL^{-1} to transmitted light in the absence of cells was 1.001 (SD 0.003) under unsaturated conditions and 0.994 (SD 0.006) under saturated conditions. For 10^8 CFU mL^{-1} the mean ratio was 1.008 (SD 0.003) and 1.001 (SD 0.003) for unsaturated and saturated conditions respectively. We concluded that cell solutions of 10^9 CFU mL^{-1} had no significant impact on water content determination by the light transmission method in our system. The light transmission efficiency appears to be affected to a greater extent by loss at interfaces between liquid, solid, and air than by attenuation in the liquid.

Example homogeneous texture experiments. Examples of CCD data obtained from a typical experiment are presented in Fig. 2.5 simply to illustrate the ability to monitor changes in microbial colonization (a & b), water content (c & d), and flow paths (e & f), over time in a noninvasive manner. The results briefly illustrated here are discussed in detail elsewhere (see Chapter 3 and Chapter 4).

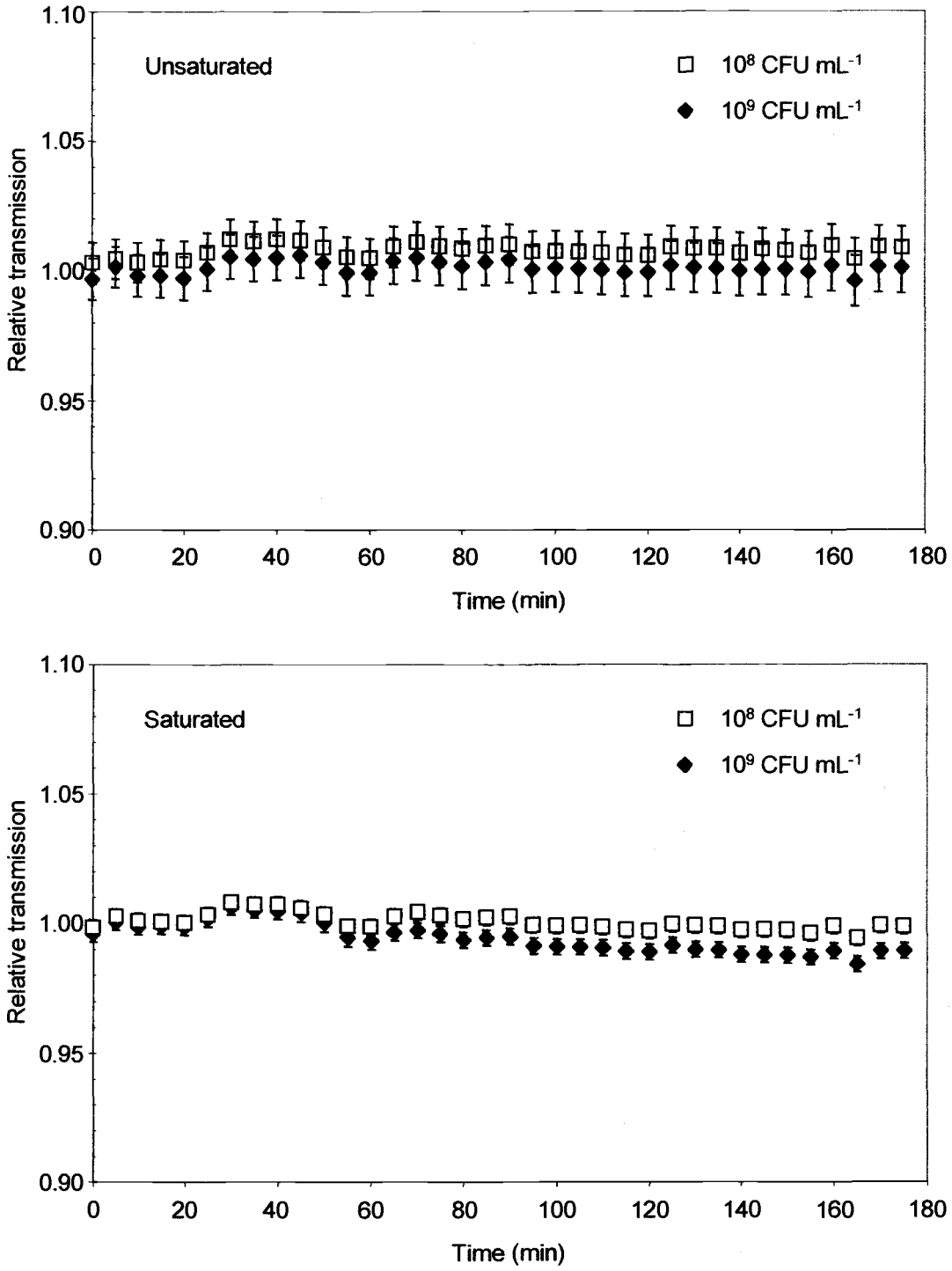

Figure 2.4. Impact of bacterial cell suspensions on light transmission. Relative transmission (compared with no cells) in unsaturated and saturated 40/50 sand.

Figure 2.5. Examples of CCD imagery. These images illustrate the spatial and temporal microbial growth expansion and accompanying changes in hydrologic properties over four days of chamber operation. Bioluminescence measurements of microbial growth and distribution (A and B); light transmission measurements of water saturation (C and D); light transmission measurements of dye pulse distribution (E and F). The first panel of each pair shows conditions on the second day, while the second panel shows conditions on the fifth day. The cross superimposed on each image indicates the point of inoculation.

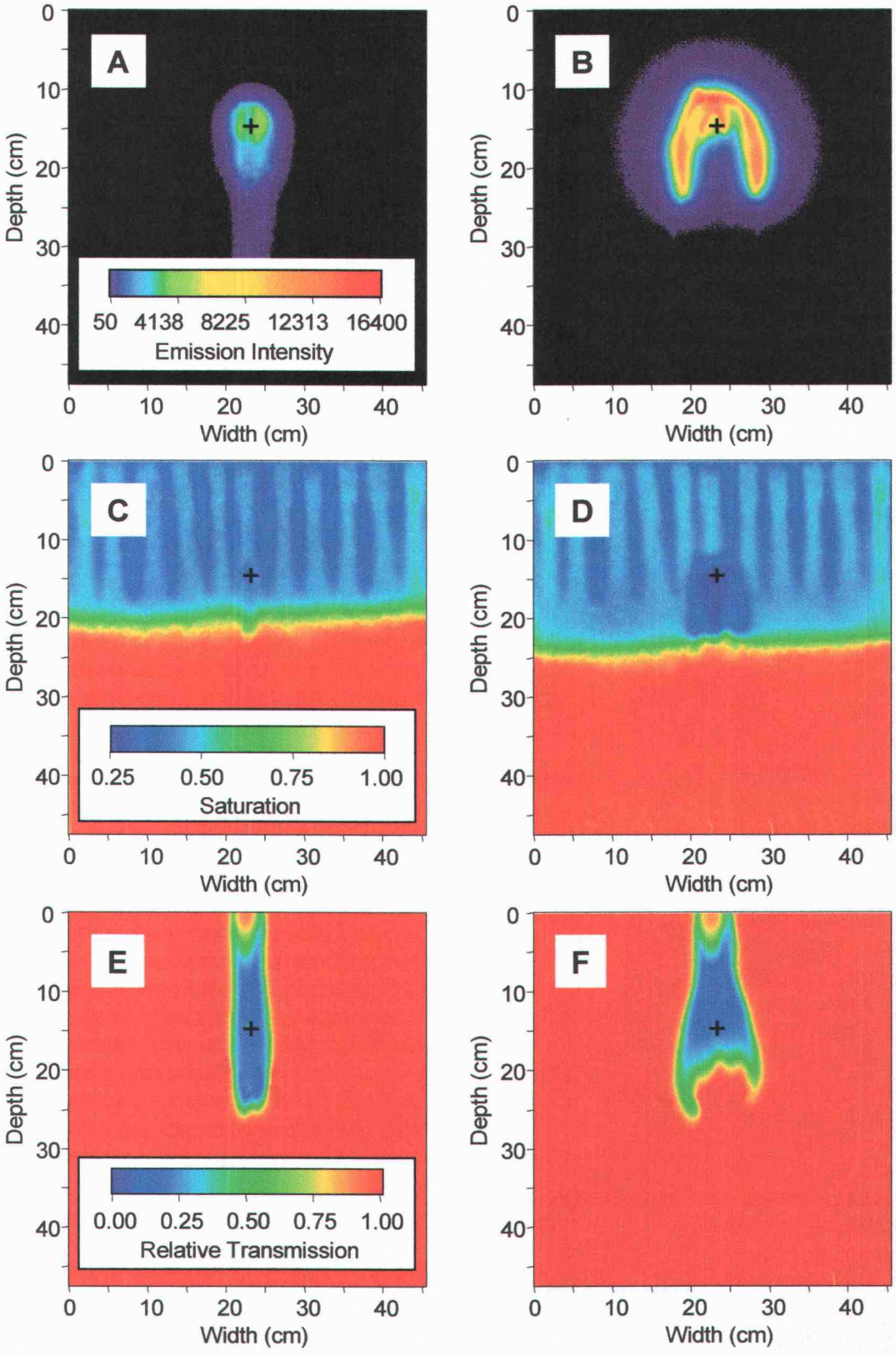
A
B
C
D
E
F
Depth (cm)
Width (cm)
0
10
20
30
40
50 4138 8225 12313 16400
Emission Intensity
0.25 0.50 0.75 1.00
Saturation
0.00 0.25 0.50 0.75 1.00
Relative Transmission

Figure 2.5.

Comparison of water content determination by light transmission and gravimetric analysis. Cell densities measured in the sand at the conclusion of the experiments described above were higher than those used to determine the impact of cell solutions on the light transmission method for measuring water content. Therefore, water content determined from gravimetric analysis of colonized sand samples was compared to water content measured by light transmission immediately prior to the end of each experiment. Results for two independent experiments are reported in Fig. 2.6. The values on the axes represent water saturation levels. The superimposed line represents a one to one correspondence. Cell density, determined by dilution plating, ranged from none detected to 9×10^{10} CFU mL^{-1} of pore water. The mean of the absolute values of the differences in saturation determined between the two methods for two independent experiments was 0.038 (95% CI 0.028 to 0.049) and 0.050 (95% CI 0.038 to 0.063) respectively. Given that some redistribution of water would be expected during the manipulations of sampling, this agreement is very good and further supports the use of light transmission in quantification of saturation in our experimental systems, even in the presence of high numbers of cells.

Summary

Digital CCD imaging of light emission (bioluminescence) permits observation of the spatial and temporal development of microbial growth, and CCD imaging of light transmission provides a simultaneous measurement of water contents and flow paths in the system. Digital CCD imaging allows for

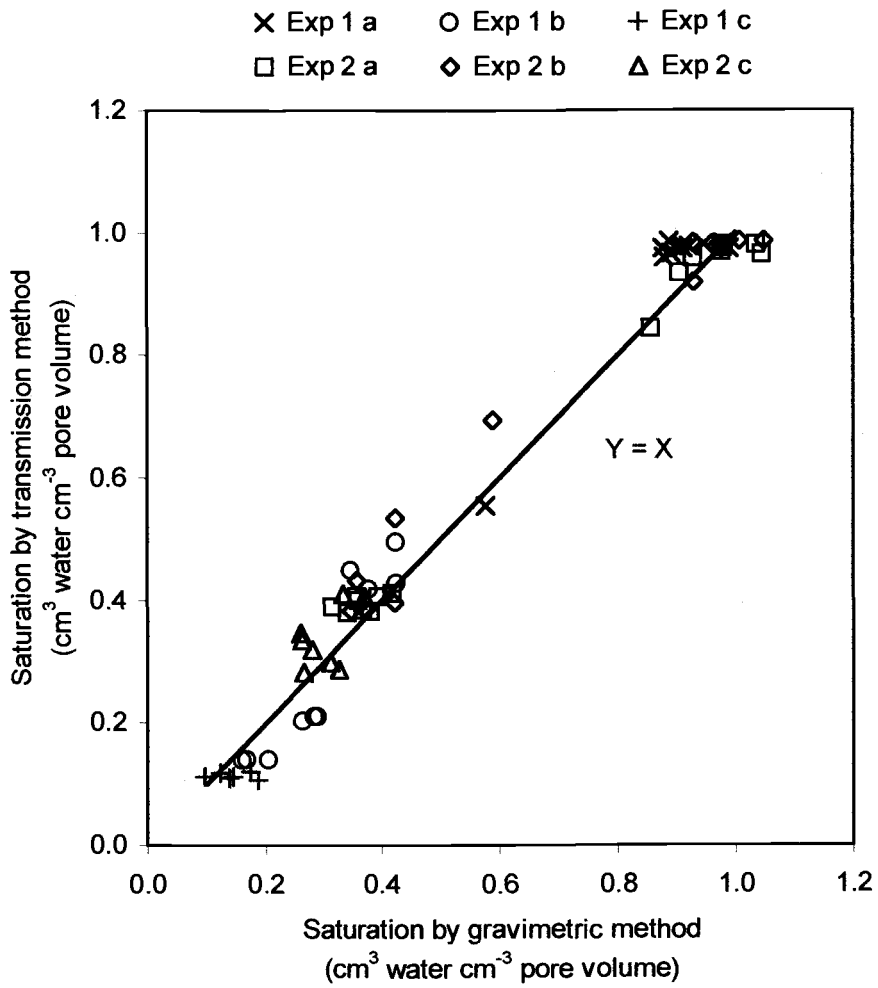

Figure 2.6. Saturation measured by light transmission and gravimetric analysis. Results are for two independent experiments (Exp. 1, n = 26; Exp. 2, n = 38). Letters in the legend indicate measured cell densities per mL of pore water (a, $< 10^9$; b, $\geq 10^9$ but $< 10^{10}$; c, $\geq 10^{10}$). Scales show level of water saturation, with a value of 1.0 indicating fully saturated. The line indicates a one-to-one correspondence.

nondestructive monitoring of the interactions of the microbial and hydrologic components of the system over time and provides an outstanding density of information at high spatial resolution. Each CCD image contains over 200,000 discrete measurements, at a spatial resolution of one millimeter.

There is an old saying: "The devil is in the details". The successful development of this experimental system involved an iterative process over a period of several years. Sterilization, packing, and inoculation protocols required several revisions before contamination problems were solved and satisfactory results were obtained. Localized subsurface point inoculation was superior to uniform inoculation of the sand where the majority of growth and activity occurred at the surface of the sand rather than within the subsurface. The system described here has the potential to be a useful tool for developing a better conceptual understanding of the interactions between microbes and their environment in the unsaturated subsurface. Recent work in the Bottomley and Selker laboratories demonstrated the ability to utilize the bioluminescence of *P. fluorescens* HK44 in response to salicylate to quantify population density in liquid culture and in saturated and unsaturated sands under static conditions (Uesugi et al., in review). That work resulted in development of a model describing the cell-density-dependent bioluminescence response that was applied to quantify population densities of *P. fluorescens* HK44 growing in the chambers under unsaturated flowing conditions (Chapter 3).

CHAPTER 3

BIOLUMINESCENCE AS A NONDESTRUCTIVE MEASURE OF MICROBIAL CELL DENSITY AND DISTRIBUTION IN UNSATURATED POROUS MEDIA

R. R. Yarwood[1], M. L. Rockhold[2], M. R. Niemet[2], J. S. Selker[2], and P. J Bottomley[1]
[1]*Department of Microbiology and* [2]*Department of Bioengineering,*
Oregon State University, Corvallis, OR 97331, USA

ABSTRACT

Glucose-dependent growth of the *luxCDABE*-containing reporter bacterium *Pseudomonas fluorescens* HK44 was followed noninvasively in a siliceous porous medium under unsaturated flow within a 45 x 56 x 1 cm two-dimensional flow cell. The spatial and temporal development of growth was mapped over the course of a one-week experiment by quantifying the daily development of bioluminescence in response to addition of the *lux*-gene inducing substrate, salicylate. A model relating the rate of increase in light-emission after salicylate exposure to microbial density successfully predicted cell densities of *P. fluorescens* HK44 over four orders of magnitude ($R^2 = 0.95$) provided that sufficient oxygen was available to permit the bioluminescence reaction to occur. Total growth predicted by the model also agreed with potential growth calculated from the mass balance of the system and previously established kinetic parameters (predicted, 1.2×10^{12} cells; calculated, 1.7×10^{12} cells). The predicted and calculated populations in the chamber at the end of the experiment were 6.0×10^{10} cells and 6.1×10^{10} cells, respectively. Light transmitted from colonized regions to uncolonized regions required identification of the spatial extent of colonization by way of a threshold. Intriguing observations included that while the rate of areal expansion of the colonized zone and the predicted populations in the newly colonized regions remained relatively constant, the proportion of potential growth that remained within the chamber declined over time. We also observed the development and

persistence of an (hypothesized) anaerobic zone associated with microbial growth in the unsaturated porous media.

INTRODUCTION

Field scale bioremediation of the vadose zone continues to be an unpredictable process, in part because of a poor understanding of the factors that influence microbial growth under conditions of unsaturated flow in the subsurface. The U. S. Department of Energy has identified as a priority research goal for the next decade the need to understand better the linkage between microbial-contaminant interactions and hydrologic processes in the subsurface (U. S. Dept. of Energy, 2000). To address facets of this issue we have developed a novel method to examine the interactions between microbial growth and solute transport under dynamic flowing conditions in unsaturated porous media. The method uses light transmission chambers to quantify pore water content and hydraulic flow paths, and bioluminescent bacteria to measure microbial activity and growth in response to solute movement.

The light transmission method for determining water content in thin slabs of porous media was introduced by Hoa (1981) and further developed by Glass et al., (1989) and Tidwell and Glass (1994). Selker (1991) extended the method to the observation of solute distribution by application of dyed solutes. Niemet and Selker (2001) made significant refinements in water content quantification in quartz sands by this method.

In recent years, bacterial *lux* genes have been used to detect and to monitor the fate of microorganisms introduced into natural environments (deWeger et al., 1991; Flemming et al., 1994a, 1994b; Rattray et al., 1990; Shaw et al., 1992), and

as an indicator of bacterial metabolic state (Duncan et al., 1994; Meikle et al., 1992). In addition, *lux*-gene fusions to inducible catabolic genes have been used to detect bioavailable concentrations of organic contaminants and heavy metals in the environment (Applegate et al., 1998; Blouin et al., 1996; Burlage et al., 1990, King et al., 1990; Heitzer et al., 1992, 1994; Selifonova et al., 1993; Sticher et al., 1997). Two recent studies have reported on the use of the *lux*-marked bacterium *Pseudomonas putida* RB1353 to monitor (point-wise, using a fiber-optic probe) bacterial activity in porous media under saturated flowing conditions (Neilson et al., 1999; Yolcubal et al., 2000). To our knowledge, no published reports exist where *lux*-gene dependent bioluminescence has been used to noninvasively quantify bacterial population growth in unsaturated porous media.

The bacterium used in this work is the bioluminescent reporter strain *Pseudomonas fluorescens* HK44 which carries a *nahG-luxCDABE* transcriptional fusion (King et al., 1990). Exposure of *P. fluorescens* HK44 to naphthalene, or its metabolite salicylate, results in induction of the *lux* system and emission of light. Recently, work in our laboratory demonstrated the ability to utilize the inducible bioluminescence response of *P. fluorescens* HK44 to quantify population density in liquid culture and in saturated and unsaturated sand under static conditions (Uesugi et al., in review). A model was developed to describe the density-dependent bioluminescence response of *P. fluorescens* HK44 in porous media.

The objectives of the work reported here were two-fold. The first objective was to use bioluminescence to monitor the spatial and temporal development of

microbial colonization under unsaturated flowing conditions. The second objective was to determine if the model of Uesugi et al. (in review) could be used to quantify microbial density during growth under unsaturated flowing conditions.

MATERIALS AND METHODS

Chamber and associated equipment

The light transmission chamber, associated equipment, and fluid application system used in this work are described in detail elsewhere (Niemet and Selker, 2001; Chapter 2). The chamber consists of two plate glass sheets separated by a U-shaped aluminum spacer, and is back-lit by a bank of fluorescent lights. When assembled, the internal chamber dimensions are 45.5 cm wide by 54 cm high by 1.0 cm thick. The fluid application system (influent manifold) contains individual syringe-needle drip-emitters. For this experiment, a manifold was used consisting of eleven 23-guage emitters spaced 4.1 cm apart. The sixth emitter was centered above the horizontal midpoint of the chamber. Feed solutions were supplied to the chamber via a multichannel peristaltic pump.

Light detection system

The light detection system in this experiment differed from that described in Chapter 2. It consisted of a thermoelectrically cooled 14-bit digital CCD camera (ISI Systems, Santa Barbara, CA) with a Kodak KAF0400 (768 x 512 pixel) scientific grade CCD array. The lens was a Nikon 35 mm, f-1.4 (Nikon

Corporation, Tokyo). Light transmission images were obtained using a 620 nm center-wavelength, 10 nm bandpass filter (Oriel model # 53930, Oriel Co., Stratford, CT) installed in the camera's internal filter wheel. Bioluminescence images were obtained using an optically clear glass filter to maintain the same overall magnification. The distance from the chamber to the lens was 3.86 m. With this system geometry, each image pixel represented approximately 0.97 mm^2 of chamber surface area. Each image provided greater than 225,000 discrete measurements over the experimental domain.

Porous medium

The porous medium used in this work was 40/50-mesh silica sand sold under the trade name Accusand® (Unimin Corp., LeSueur, MN). The physical, chemical, and optical properties of this material have been well characterized (Schroth et al., 1996, Niemet and Selker, 2001). Sand was prepared by first soaking in a 5 M NaCl solution followed by a thorough rinsing with distilled water. This treatment allowed the removal of fine particulates. The washed sand was autoclaved three times for one hour each time, and allowed to stand at room temperature for at least 24 hours between each sterilization. After autoclaving for the third time, the sand was oven dried to constant weight at 50°C.

Bacterial strain and growth conditions

Pseudomonas fluorescens HK44 was kindly supplied by Gary Sayler, University of Tennessee, Knoxville, TN. *P. fluorescens* HK44 hosts the plasmid

pUTK21 containing the *luxCDABE* gene cassette and a tetracycline resistance marker (King et al, 1990). All liquid media was supplemented with 15 mg L^{-1} tetracycline (Tet15). Working stocks were maintained on plates of half-strength TSB (Difco Laboratories, Detroit, MI) supplemented with 15 mg L^{-1} tetracycline and 1.5% (w/v) Bacto Agar. The liquid medium used in the experiment was a nitrate-free minimal mineral salts (MMS) (Chapter 2). Glucose at 250 mg L^{-1} (Glu250) was applied through the central dripper only. Salicylate, at 100 mg L^{-1} (Sal100), was used to induce the bioluminescent response.

Preparation, packing, and inoculation

The front sheet of chamber glass was drilled with a series of nine ports in an inverted T configuration (see the first panel in Fig. 3.1). The ports were sealed with high temperature silicon rubber to act as septa for injection or sampling via syringe. Preparation of materials and chamber packing were carried out as described in Chapter 2. Sand was added to a height of 48 cm above the surface of the effluent manifold screen. The calculated porosity of the sand pack was 0.332.

Prior to saturation, the chamber was purged through the lower port with 0.2 μm filtered CO_2 gas to displace all of the air within the pore space of the sand. Because CO_2 is more water-soluble than air, this treatment minimized entrapped gas as the chamber was filled with liquid. About seven pore volumes of MMS were pumped through the system (from the bottom of the chamber and siphoned off at the top) to remove CO_2 from the system.

P. fluorescens HK44 was grown overnight with shaking (150 rpm) at 27°C in MMS+Tet15 supplemented with 1.0 g L^{-1} glucose. The culture was centrifuged, washed with MMS basal medium, and resuspended to 5 x 10^8 CFU mL^{-1} in MMS+Tet15+Sal100 to induce the bioluminescence response. After the culture was visibly bioluminescent, 5.0 mL was injected into the saturated sand through a port in the front glass sheet of the chamber at a depth of 15 cm below the surface. This resulted in an inoculated region with a circular surface area of 4.4 cm in diameter and bulk volume of approximately 15 cm^3. After one hour, the influent flow was started, and the effluent port was opened to allow the chamber to drain. The flow rate per individual dripper was 28.7 ± 0.4 mL h^{-1} (overall flow rate 315.6 ± 4.6 mL h^{-1}). The open end of the effluent tube was positioned just above the level of the upper surface of the effluent manifold screen to set the lower zero-pressure boundary at about one cm above the lower edge of the sand pack. Under these conditions the capillary fringe rose to slightly below the vertical midpoint of the sand pack. The upper half remained unsaturated, with a volumetric water content of about 0.12 cm^3 cm^{-3}.

Data collection and analytical methods

Liquid saturation. Light transmission images were collected several times each day and water saturation levels were determined by the method of Niemet and Selker (2001). Exposures of 0.8 s were made at an aperture setting of f-1.4 and with the 620 nm-centered 10 nm-bandpass filter.

Bioluminescence. The bioluminescence response was measured once each day as follows. The influent drip emitters were switched to a solution of MMS+Tet15+Sal100, except for the central dripper, which was switched to a solution of MMS+Tet15+Glu250+Sal100. Salicylate was applied onto the chamber for 150 min, and then the feed system was restored to the standard solutions. The bioluminescence response was recorded in a series of images (10 min exposure, f-1.4) taken at 20-minute intervals with the clear filter in place of the 620 nm filter to maintain a consistent optical path.

Effluent and pore liquid sampling. Effluent samples were analyzed for biomass protein and for glucose. The entire first 1100 mL of chamber effluent was collected to insure capture of the portion of the inoculated cells initially washed from the sand. Subsequently, 35 mL aliquots of chamber effluent were obtained at intervals throughout the course of the experiment. Cells were collected by centrifugation, washed with MMS and resuspended in 1.0 mL of MMS. The first supernatant fraction and the resuspended cell pellets were stored at -20°C and analyzed later (three analytical replicates) for glucose and protein using anthrone (Brink et al., 1960) and bicinchoninic acid (BCA) respectively. The Micro BCA protein assay kit (Pierce, Rockford, IL) was employed for protein measurements.

Samples of pore liquid were obtained from each of the five lower sampling ports in the chamber front glass sheet at intervals throughout the experiment and analyzed for dissolved oxygen concentrations. Samples were withdrawn very slowly to minimize any effect on the chamber water content. Dissolved oxygen

was determined using a YSI model 5300 Biological Oxygen Monitor (Yellow Springs Instrument Co., Yellow Springs, OH) equipped with a YSI model 5331 Clark-type oxygen microelectrode and a 1.8 mL water-jacketed sample chamber.

Final destructive sampling of the sand. At the end of the experiment, the chamber contents were destructively sampled and analyzed for biomass, total neutral carbohydrate, and gravimetric water content distributions. Samples (2.5 x 2.5 x 1.0 cm) of chamber contents were aseptically collected according to a predetermined grid pattern. A CCD image of the grid provided a reference between image data and sampling data. Within a few hours of the end of the experiment, sand samples were analyzed for biomass and gravimetric liquid content. Weighed samples were added to 1.5 mL microfuge tubes and cells extracted into 0.5 mL MMS by gentle vortexing (30 s). Biomass was quantified in dilutions of the sand extracts both by viable plate counts (VPC) and protein analysis (see above). Viable plate counts were carried out on half-strength TSB agar supplemented with 15 mg L^{-1} tetracycline.

Quantification of the population with bioluminescence. Uesugi et al. (in review) developed a model relating cell density to the rate of increase in the rate of light production after exposure to the inducer. For cells in the presence of sand, the model is expressed in the equation:

$$(L/c)^{1/2} = tn\phi(\theta)(B'/2)^{1/2} \qquad (1)$$

where L is light units per minute (LUPM) (CCD counts divided by the exposure time in minutes), c is the *P. fluorescens* HK44 cell density in CFU mL^{-1} of pore

liquid, t is the time in minutes since exposure to salicylate, and B' is the rate of increase in cellular light production rate with units of (LU / [cell-min^2]). The term $n\,\phi(\theta)$ incorporates the attenuating effects of porosity, n, and the effect of variations in volumetric water content, $\phi(\theta)$, on light detected from the sand. The $\phi(\theta)$ relationship was determined empirically (Uesugi et al., in review). The linear portion of a plot of $(L/c)^{1/2}$ versus t has the following slope, m:

$$m = n\phi(\theta)(B'/2)^{1/2} \qquad (2)$$

Solving equation (2) for B' gives:

$$B' = 2[m/(n\phi(\theta))]^2 \qquad (3)$$

When B' is known, the following expressions equivalent to equations (1), (2), and (3) can be used to solve for cell density, c.

$$(L/B')^{1/2} = tn\phi(\theta)(c/2)^{1/2} \qquad (4)$$

$$m = n\phi(\theta)(c/2)^{1/2} \qquad (5)$$

$$c = 2[m/(n\phi(\theta))]^2 \qquad (6)$$

In the experiments of Uesugi et al. (in review), which were carried out in batch reactors with non-growing cells under non-flowing conditions, the induction time, t, for any given image was constant for the entire imaged area. The volumetric water content, θ, used to obtain $n\,\phi(\theta)$, was also constant. Under the conditions of unsaturated flow reported here, however, water content varies with position in the chamber and time of first exposure to salicylate varies both with position and water content. The water content, and thus the $n\,\phi(\theta)$ term, for any

position in the chamber can be obtained from a saturation image obtained using the light transmission method taken at about the same time as the emission images (i.e. just prior to the start of salicylate application). A reasonable value for the induction time, t, at a given position can also be obtained using the same saturation image by assuming a uniform flow field across the width of the chamber and applying the following 1-D travel time equation:

$$T = z\theta/q \qquad (7)$$

where T is the travel time in minutes, z is the depth in cm, θ is the pixel-row-averaged water content at that depth, and q is the areal flux rate in cm min^{-1}. In the work reported here, there was a two-minute delay (D) between the time the salicylate pulse was started and salicylate first reached the surface of the sand. This represented the time required for salicylate to travel through the influent lines to the drippers. The total travel time to move from the sand surface to the effluent manifold was 135 min. The induction time, t, for a given exposure becomes:

$$t = (TSC - D) - T \qquad (8)$$

where TSC is the elapsed time in minutes (at shutter-closing) since the start of the pulse. Substituting equation (7) into equation (8) gives:

$$t = (TSC - D) - (z\theta/q) \qquad (9)$$

The B' values have dimensions of light units and thus are a function of camera sensitivity and position of the experimental system in relation to the camera. Therefore, we determined the value for B' appropriate for our system

independently using the relationship described by equation (1) and experimentally measured values for population density determined by destructive sampling and the day 7 light emission data. Sixteen samples from the brightly glowing regions of the colony were selected. These samples represented volumetric water contents ranging from 0.11 to 0.33 cm^3 cm^{-3}, and cell densities ranging over four orders of magnitude. The results are presented in Table 3.1. The mean value for B' was found to be 12.1 x 10^{-10} (95% CI 8.4 x 10^{-10} to 15.8 x 10^{-10}).

Image analysis. Digital image processing was performed using Transform 3.4 (Fortner Software LLC, Sterling, VA) as described previously (Chapter 2).

RESULTS

Spatial development of colonization

Figure 3.1 shows the daily maximum bioluminescence for each day of the experiment. The image for day 1 was taken immediately after inoculation and shows the initial distribution of cells before flow was started. Microbial colonization spread from the 4.4 cm diameter inoculated region on day 1 to cover a region of >17 cm in width by day 7. Between day 5 and day 7 a finger of colonization advanced upward against flow, migrating a distance of 3 cm by the end of the experiment. On day 2, aqueous phase cells transported by the downward flow were clearly visible as streams of bioluminescence in the water-saturated region below the colonized zone. On subsequent days, light emission from the chamber was only observed in the unsaturated region. However, bioluminescence

Table 3.1. Determination of B' value.

Volumetric moisture ($cm^3\ cm^{-3}$)	Measured population (CFU mL^{-1}) ($x10^{10}$)	Slope ($x10^{-6}$)	R^2	B' ($x10^{-10}$)
0.14	0.060	0.88	0.98	7.5
0.16	0.64	1.11	0.98	9.2
0.15	0.13	0.91	0.98	7.6
0.15	1.9	0.69	0.97	4.2
0.15	1.4	1.38	0.98	16.4
0.14	0.56	1.34	0.98	18.2
0.13	5.9	0.78	0.96	8.2
0.13	6.2	0.77	0.96	8.5
0.14	0.030	1.66	0.98	27.1
0.11	9.8	0.50	0.96	4.8
0.12	1.6	1.08	0.97	18.4
0.11	2.2	0.44	0.96	4.0
0.15	0.077	1.18	0.99	11.7
0.15	0.44	1.65	0.98	24.1
0.19	0.29	1.69	0.96	12.7
0.33	0.00069	3.10	0.99	11.6

Samples (n = 16) were obtained from brightly glowing regions of the colonized zone. The slope and R^2 values are for a plot of $(L/c)^{1/2}$ against time (see text). B' mean value: 12.1×10^{-10} (95% CI 8.4×10^{-10} to 15.8×10^{-10}).

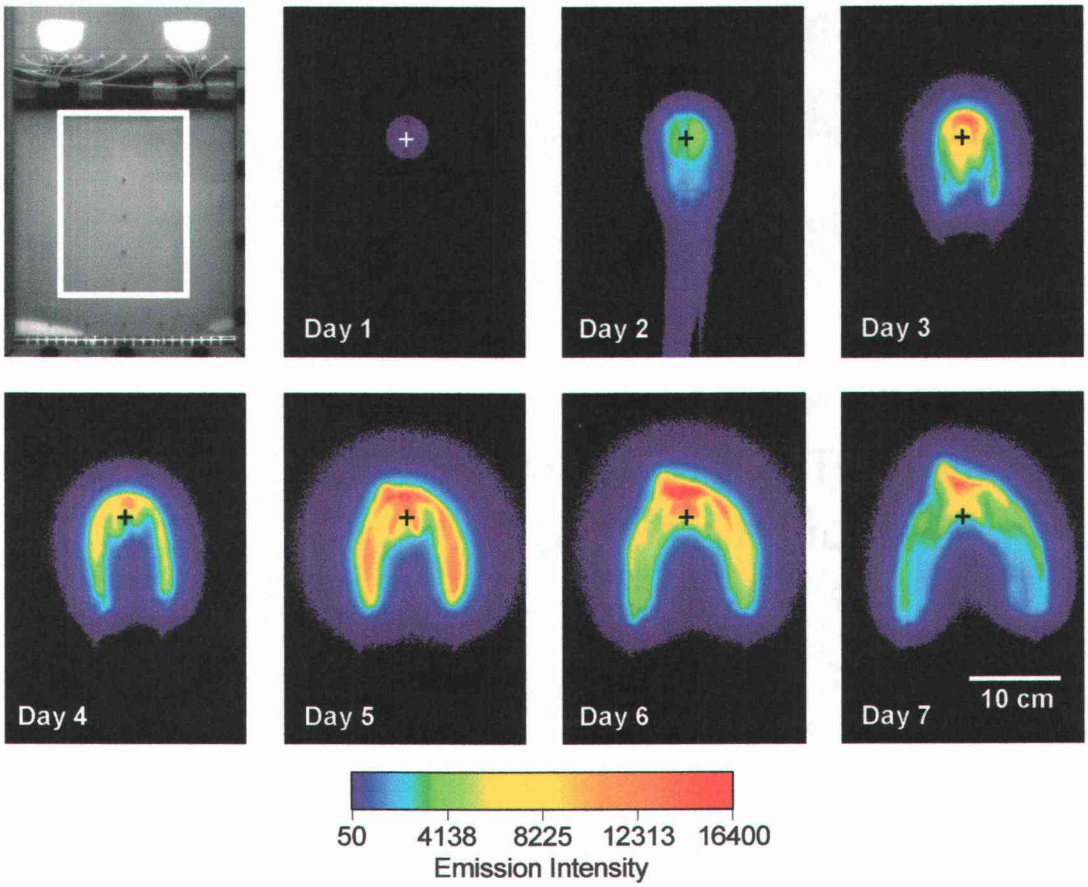

Figure 3.1. Daily maximum bioluminescence. The first panel shows a view of the chamber under room lighting. The superimposed rectangle defines the region of the chamber shown in each of the subsequent panels. The images have been artificially colorized to clearly show differences in emission intensity (LU, arbitrary light units) during each 10-minute exposure. The cross superimposed on each image indicates the location of the inoculation port, also visible as the uppermost port in the first panel (look for inverted-T shape).

was restored in the effluent upon exposure to air as it exited the chamber. By day 4, the interior region of the colonized zone no longer responded to the application of salicylate. This pattern prevailed for the remainder of the experiment.

Downstream dissolved oxygen

Corresponding downstream dissolved oxygen concentrations are presented in Fig. 3.2. The horizontal axis indicates the position of each sampling port with respect to the vertical centerline of the chamber. Oxygen was depleted most rapidly and extensively directly below the colony, declining to less than 2 mg L^{-1} by the second day of the experiment. The zone of oxygen depletion expanded outward with time, paralleling the expansion of the colonized region.

Light response profiles

Figure 3.3 shows the day 7 bioluminescence response profiles for eight 2.5 cm by 2.5 cm sectors along a vertical transect through the colonized zone. Light units (LU) are the mean values accumulated over each 10 min exposure for the 625 pixels within each of the sectors. Time zero indicates the start of the 150-minute salicylate pulse. The elapsed time before emission detection, peak emission level, and time of peak emission all varied with depth through the colonized region. For example, light emission from the upper three sectors (A through C) exceeded 50 LU at 45 min after salicylate addition. The time increased by 20 min for each of the next four lower sectors (D through G). Emission for the

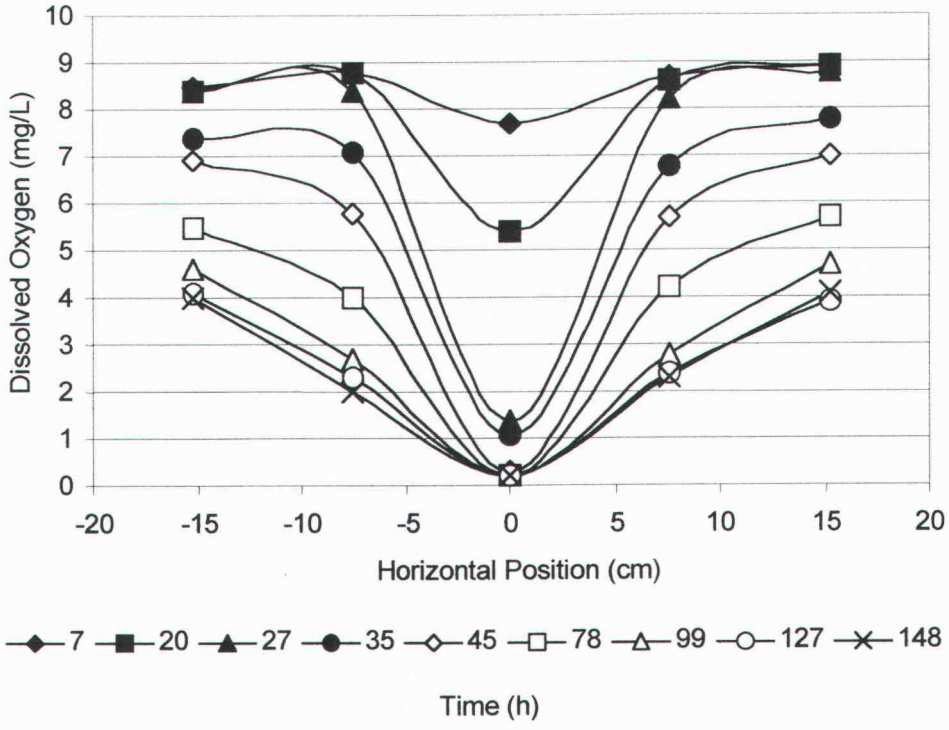

Figure 3.2. Downstream dissolved oxygen. The horizontal axis indicates the position of each sampling port with respect to the vertical centerline of the chamber. The legend values indicate elapsed time (h) after the start of the experiment.

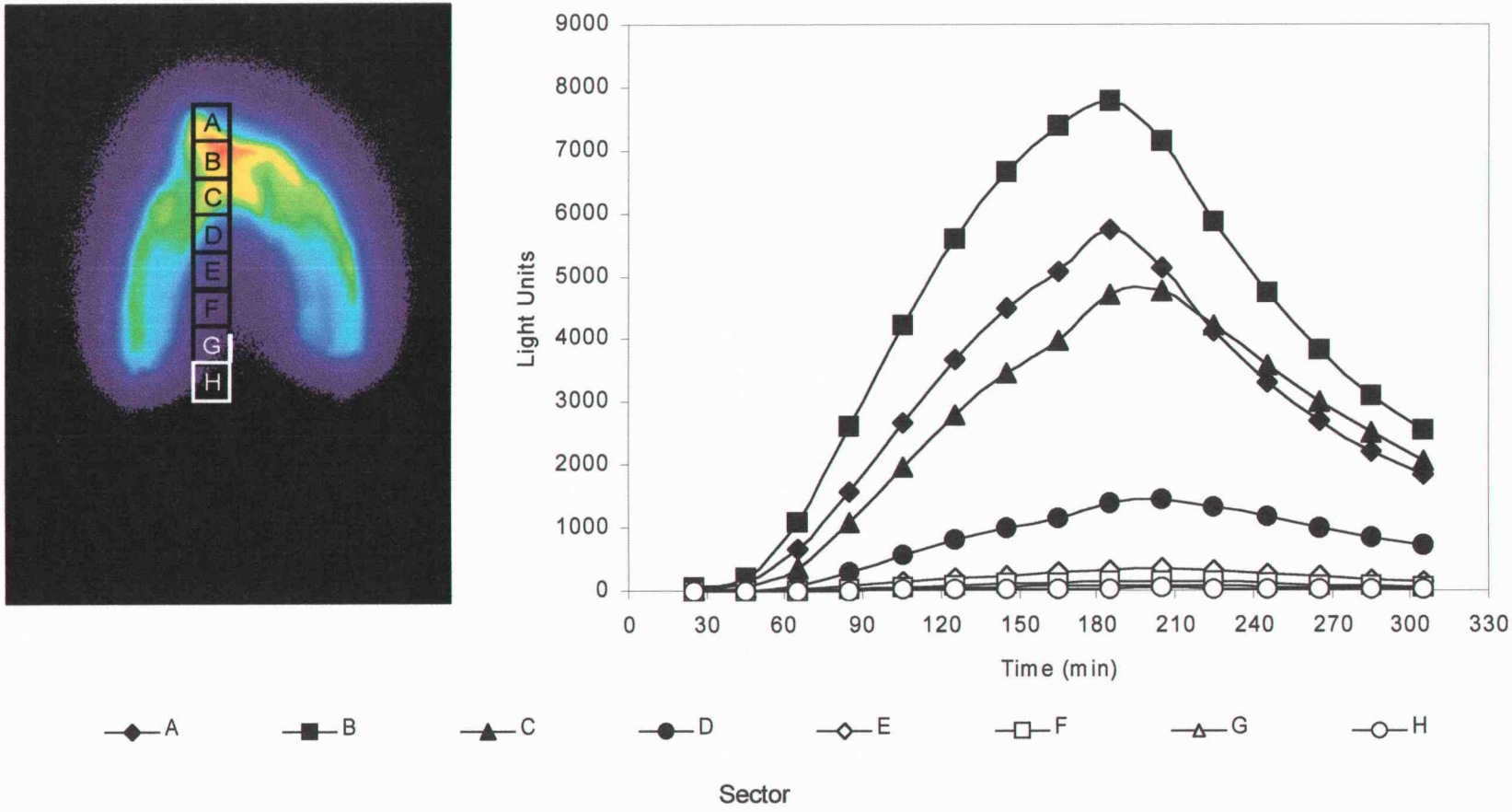

Figure 3.3. Typical bioluminescence response profiles. Light levels are the mean values for day 7 accumulated over each exposure for the 625 pixels within each of the 2.5 cm by 2.5 cm regions indicated in the first panel. Time zero indicates the start of the 150-minute salicylate pulse.

lowest sector did not reach 50 LU until 205 min after the start of the salicylate pulse. Peak emission levels varied over two orders of magnitude, with a high of 7800 LU (sector B) and a low of 50 LU (sector H). Peak emission was recorded at 185 min for the upper two sectors (A and B) and at 205 min for the lower eight sectors (C through H). After salicylate was removed from the system, light emission declined in a logarithmic fashion. The half-life for light emission decay was 78.6 min (95% CI 76.0 to 81.4 min) determined over all 57 sectors where the sector mean light emission reached a maximum of at least 100 LU (10 LU min^{-1}).

Defining the extent of colonized area

Light emitted by the cells travels in all directions, not just towards the camera. This light is reflected and refracted at interfaces of air, water, and glass within the imaged area and can be seen away from the colonized area as a smoothly changing low level signal. As emission increases at a given point, the intensity of an apparent halo of light about this point also increases (referred to herein as the lantern effect). It is necessary, therefore, to delineate the borders of the colonized zone to avoid over estimating the amount and extent of biological activity.

Figure 3.4a shows an emission profile for a horizontal transect through the colonized zone at a depth of 15 cm (the inoculation depth) taken on day 3 of the experiment. The panel shows the emission for the fifth image of the salicylate pulse. The criteria for using the fifth image is that it falls within the middle of the increasing portion of the bioluminescence response curve, all regions of the chamber have had sufficient time for induction, and salicylate is still present

Figure 3.4. Defining the extent of the colonized area. Panel A shows the emission profile for a horizontal transect through the colonized zone at a depth of 15 cm on day 3 to illustrate the method used to determine the boundary of the colonized zone (see text).
a. inferred area of colonization
b. lantern effect
Panel B shows the development of the colonized region with time. The outermost, dashed line represents a level of 100 light units on day 7 and illustrates the potential for error in defining the extent of colonization if the lantern effect was not accounted for.

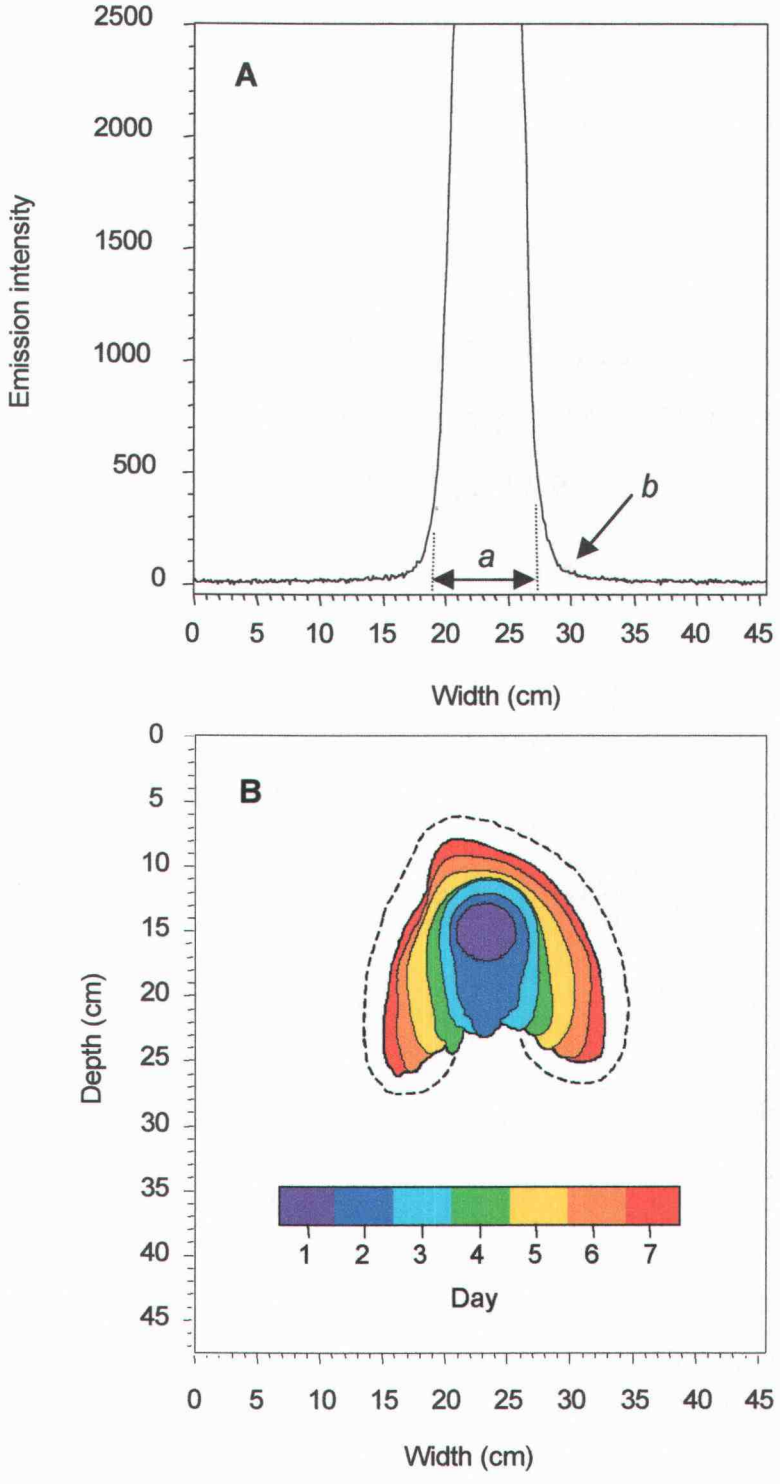
A
Emission intensity
2500
2000
1500
1000
500
0
a
b
0 5 10 15 20 25 30 35 40 45
Width (cm)
B
Depth (cm)
0 5 10 15 20 25 30 35 40 45
1 2 3 4 5 6 7
Day
0 5 10 15 20 25 30 35 40 45
Width (cm)

Figure 3.4.

everywhere in the chamber. A similar profile was generated for each day of the experiment. The nearly vertical portion of each side of the curve was extrapolated to the baseline to define the edge of the colonized zone. The observed emission intensities at these points for the right and left sides were then averaged to obtain a threshold value for a given day. The threshold value was used to generate a contour line defining the boundary of the colonized zone. Positions within the chamber with light levels below these threshold values were considered to be "uncolonized". Stacking of the daily perimeter threshold plots reveals the development of the colonized region with time (Figure 3.4b). Moving from the middle outward, the contour lines represent the maximum extent of the colony on subsequent days. The outermost, dotted line on the figure represents a level of 100 LU in the maximum emission image on day 7, to show the lantern effect.

The number of pixels contained within each of the regions was used to calculate the changing area of the colony on each day (Table 3.2). The colonized area increased from 15.8 cm^2 on day one to 224.8 cm^2 on day 7. The average rate of increase in the colonized area was relatively constant (34.7 ± 7.2 cm^2 day^{-1}).

Quantification of the population with bioluminescence

Figure 3.5 shows the population density (log CFU mL^{-1}) predicted by the model for density-dependent bioluminescence using day 7 emission data compared to population density (log CFU mL^{-1}) measured on day 7 after destructive sampling. The comparison was made for 19 samples obtained from brightly glowing regions of the colonized zone, where oxygen was assumed to not be

Table 3.2. Daily expansion of colonization and model-predicted populations by region.

	Colonized area		Predicted population by region ($CFUx10^{10}$)							
Day	Total (cm^2)	Change ($cm^2\ d^{-1}$)	1	2	3	4	5	6	7	
1	15.8 [a]									
2	54.7	38.8	5.7	5.3						
3	83.7	29.0	13.1	12.9	3.6					
4	106.8	23.1	7.3	7.2	7.5	4.2				
5	150.7	43.8	30.9[b]	18.4[b]	19.7[b]	15.8[b]	19.0			
6	191.5	40.8	14.2	13.4	15.3	10.6	21.9[b]	9.3		
7	224.4	32.9	7.0	7.8	9.3	5.5	15.3	11.1[b]	4.1[b]	
		Avg. (SD)	[b]Maximum predicted population							Sum[c]
		34.7 (7.2)	30.9	18.4	19.7	15.8	21.9	11.1	4.1	121.8

Data represent the total and daily change in colonized area, and the bioluminescence-predicted populations in each of the regions of the colonized zone that were previously defined in Fig. 3.4b.

a. inoculum

b. maximum bioluminescence model-predicted population per region

c. sum of maximum model-predicted values for all regions

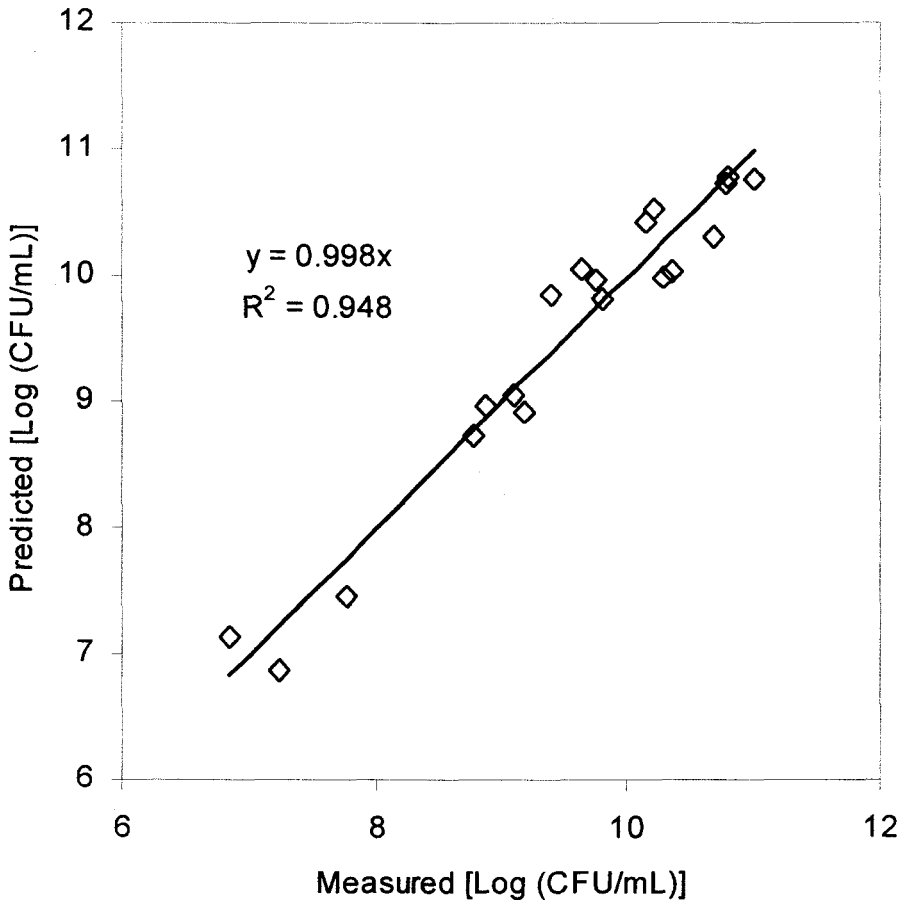

Figure 3.5. Model-predicted and measured population densities. Data represent 2.5 by 2.5 cm samples (n = 19) from brightly glowing regions of the colonized zone.

limiting. The slope of the fitted regression line was 0.998 (95% CI 0.985 to 1.012) with an R^2 of 0.948.

The average B' value (12.1×10^{-10}, see Materials and Methods) determined from the day 7 light emission data and population density measured after destructive sampling was used to apply the model to predict population densities for earlier days in the experiment. The bioluminescence data were transformed with the relationship $(L/B')^{1/2}$. The corresponding light transmission images for water content were transformed into a series of data sets representing the time, t, elapsed since first exposure to salicylate for each position in the domain using the relationship defined by equation (6). The same light transmission images were also transformed into data sets containing the water-content related correction associated with each position in the domain ($n\,\phi(\theta)$). Next, the $(L/B')^{1/2}$ data sets and the time (t) data sets were used to construct a series of data sets containing the slope values m for B' by linear regression. Finally, equation (9) was used to construct a data set containing the predicted population density in CFU mL^{-1} of pore liquid for each position in the domain, using the slope (m) data sets and the water correction ($n\,\phi(\theta)$) data sets. Further transformations allowed the expression of the predicted population in terms of CFU (cm^{-3}) of pore volume, or CFU g^{-1} of dry sand.

Table 3.2 shows the predicted population corresponding to the regions shown in Figure 3.4b for each day of the experiment. With the exception of day 5, predicted cell numbers per cm^2 in the newly colonized regions remained relatively

constant throughout the course of the experiment ($1.5 \pm 0.4 \times 10^9$ CFU cm^{-2}, omitting day 5). Predicted populations increased in the immediately adjacent "one-day-old" regions as well, but generally decreased in regions "two-days-old" or older than the newly colonized region. The bioluminescence reaction requires oxygen, therefore a decrease in predicted population for a given region might be an artifact of quenching of the light reaction due to oxygen depletion, and this was assumed to be the case. Therefore, the sum of the maximum predicted population for each region identified in Fig. 3.4b was used to calculate the total number of cells predicted to have been grown during the experiment. The total production predicted by the bioluminescence model as described above was 1.2×10^{12} cells. The model-predicted population in the chamber on day 7, based on the sum of the predicted populations for the seven regions of the colonized zone was 0.6×10^{12} cells. The latter value may be an underestimate, because it does not include the population of cells in the dark interior region of the colony that did not respond to salicylate.

Growth predicted by bioluminescence was compared with potential growth based on previously determined kinetic parameters and measured effluent glucose and biomass protein. The potential growth per day based on the mass balance is presented in Table 3.3. The proportion of daily potential production associated with the sand declined from 96.7% on day 2 to 12.7% on day 7. The slope of a plot of $\log_{10}$ of that proportion against time was -0.19 ($R^2 = 0.98$). Overall, 64.8% of the calculated potential production was recovered in the effluent. The total glucose

Table 3.3. Potential growth based on mass balance.

	Measured quantities (mg or CFUx10^{10})			Inferred potential production (mg biomass or CFUx10^{10})					
				Total		Sand-associated			
						New[c]		Cumulative	
Day	Glucose consumed[a] (mg)	Effluent cells[b] (mg)	(CFU)	(mg)	(CFU)	(mg)	(CFU)	(mg)	(CFU)
2	33.3	0.6	0.2	18.0	6.7	17.4	6.5	17.4	6.5
3	128.4	14.2	5.3	69.3	25.9	55.1	20.6	72.5	27.1
4	155.6	46.4	17.3	84.0	31.3	37.6	14.0	110.1	41.1
5	169.9	68.9	25.7	91.7	34.2	22.8	8.5	132.9	49.6
6	171.2	75.6	28.2	92.4	34.5	16.8	6.3	149.7	55.9
7	202.7	95.6	35.7	109.5	40.9	13.9	5.2	163.6	61.0
Sum	861.1	301.3	112.3	464.9	173.5				

Parameters used: growth yield on glucose, 0.54; cell dry wt. 2.7×10^{-13} g; cell composition 55% protein.

a glucose input minus glucose measured in effluent

b. based on measured effluent total cell protein

c. total daily potential growth minus daily measured effluent cells

input was 1064 mg and 203 mg was recovered in the effluent, indicating that 861 mg of glucose was metabolized. The total biomass protein (as mg BSA equivalents) recovered in the effluent was 166 mg. In previous column experiments with the same flow rates and substrate loading conditions used in the current experiment, the yield of *P. fluorescens* HK44 was determined to be 0.54 ± 0.2 (mg dry cells mg glucose^{-1}) (data not shown). In previous batch experiments the cell dry weight for *P. fluorescens* HK44 was determined to be 2.7 x 10^{-10} mg, and protein comprised 55% of the dry weight (data not shown). Given the glucose consumption during the present experiment, and a yield coefficient of 0.54, the potential cell production was 465 mg, or the equivalent of 1.7 x 10^{12} cells. Subtracting the effluent biomass (166 mg protein, or 302 mg of cells) from the potential production leaves 163 mg of cells associated with the sand at the end of the experiment, or the equivalent of 0.6 x 10^{12} cells. Both the total potential production and the potential number of cells in the chamber on day 7 agree well with the results for model-predicted growth.

Development of an anaerobic zone in unsaturated media

Figure 3.6 shows the relationship of the emission intensity on day seven and measured population density with distance from lower left to upper right along the indicated transect. Population density was determined on sand samples obtained by destructive sampling of the chamber a few hours after the bioluminescence image was obtained. Emission intensity represents the sum for each indicated sector over all emission images made on that day. Population density is reported as colony

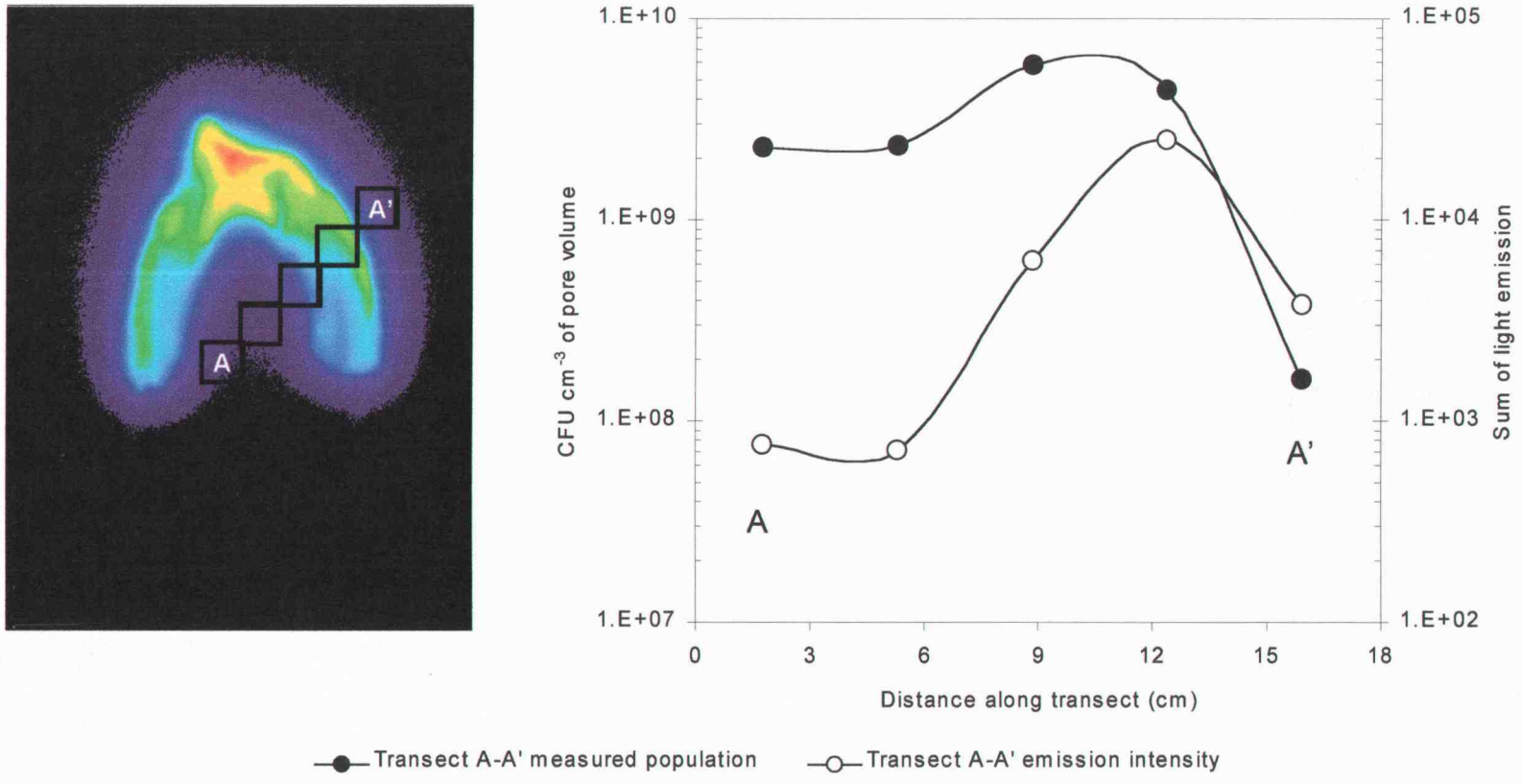

Figure 3.6. Emission intensity and population in interior of colonized zone. Data represent the measured day 7 population density and corresponding day 7 bioluminescence response along the indicated transect. Emission intensity is given as the sum for each indicated sector over all emission images made on that day. Distance represents the midpoint distances between the 2.5 cm by 2.5 cm sectors.

forming units (CFU) per cm^3 of pore volume. The distance represents the midpoint distances between the 2.5 cm by 2.5 cm sectors. Plate counts and protein analysis revealed that sufficient numbers of viable bacterial cells existed in the dark interior region of the colonized zone to produce a strong bioluminescent response. The stability of the bioluminescent phenotype in the population of the dark region was verified by observation of light emission after exposing the plated colonies to naphthalene vapors. The absence of bioluminescence in the interior region of the colonized zone in conjunction with the downstream dissolved oxygen data (Fig. 3.2) suggests that anaerobic conditions were established and maintained within the colonized zone despite the fact that the sand was unsaturated and that fresh liquid medium was continuously supplied to the chamber.

DISCUSSION

Chapter 2 described the development of a two dimensional system for studying the interactions of the microbiologic, hydrologic, and physical components of the unsaturated subsurface through the use of light transmission chambers and CCD imagery. Here has been shown the ability to quantify the development of microbial growth under unsaturated flow by monitoring bioluminescence in response to periodic additions of an inducing substrate.

The application of a nonlinear model to describe the relationship between the rate of increase in light production with time to population density developed by Uesugi et al. (in review) gave a good fit between predicted population density

based on bioluminescence and measured population density of colonized regions where oxygen availability and metabolic state were assumed to be non-limiting. Several studies have reported a linear relationship between light emission and cell density either when the bioluminescence was measured at a fixed time point after induction or when peak bioluminescence was related to cell concentration (Neilson et al., 1999; Rattray et al., 1990; Yolcubal et al., 2000). Although Neilson et al. (1999) found a strong relationship ($R^2 = 0.997$) between peak bioluminescence and cell density, the time required to reach peak bioluminescence also varied with cell density (between two and eight hours). To quantify density in a dynamic system, it is important to obtain measurements as quickly as possible. The necessity of waiting several hours to capture the peak of bioluminescence may lead to complications due to changes occurring in the system (such as in population densities, oxygen levels, and water contents) over shorter timescales than that required to obtain the bioluminescence data. The relationship between the rate of increase in light production and cell density permits measurements to be made more quickly. Cells need only be exposed to inducer for sufficient time to determine the rate of increase in light emission.

There are some limitations with the model since it tends to over-predict colonization in sectors just outside the colony due to the lantern effect described in the results. Light transmitted from colonized regions to uncolonized regions requires identification of the spatial extent of colonization by way of a threshold. Further, the magnitude of colonization was under-predicted in sectors below the

colony, apparently due to oxygen limitation. Under conditions where oxygen is sufficient, the model successfully predicted cell densities over four orders of magnitude. Predictions of *P. fluorescens* HK44 population growth based on the bioluminescence model over the course of the experiment were in good agreement with calculations based on the mass balance for this experiment and on the potential growth determined from parameters obtained in previous experiments with under similar conditions of flow and substrate loading.

It was interesting to observe that while the rate of areal expansion of the colonized zone and the predicted populations in the newly colonized regions remained relatively constant, the proportion of daily potential growth that remained within the chamber declined over time. Furthermore, populations continued to increase in the "one-day-old" colonized regions, indicating that glucose and oxygen delivery to these regions was maintained. These observations raise some interesting questions. We did not determine from where within the colonized zone the effluent cells originated. Perhaps they were actively growing cells released into the aqueous phase through the process of cell division, or attached cells detached from sand due to shear forces. On the other hand, they may have been less metabolically active cells originating from regions of the colonized zone where glucose and/or oxygen were limited. Others have reported that starvation conditions may stimulate detachment of attached cells (e.g. Allison et al., 1998).

Finally, the observation of the development of the dark interior region of the colony points out the potential usefulness of bioluminescence to map the location

and spatial and temporal development of aerobic and anaerobic zones in this dynamic experimental system. Ideally, a second marker that is not dependent on these conditions would be available to obtain data on microbial distribution, while the *lux* system would be employed as an indicator of cell status and oxygen availability. To this end, we are developing green fluorescent protein (GFP) and GFP/*lux*-marked organisms that will permit independent observation of both microbial distribution and O_2-dependent activity.

CHAPTER 4

IMPACT OF MICROBIAL GROWTH ON WATER FLOW AND SOLUTE TRANSPORT IN UNSATURATED POROUS MEDIA

R. R. Yarwood[1], M. L. Rockhold[2], M. R. Niemet[2], J. S. Selker[2], and P. J Bottomley[1]
[1]*Department of Microbiology and* [2]*Department of Bioengineering,*
Oregon State University, Corvallis, OR 97331, USA

ABSTRACT

A novel analytical method was applied that allowed for continuous observation of microbial development while simultaneously monitoring hydrodynamics in porous media in a two-dimensional system under unsaturated flowing conditions. Bioluminescence was used to monitor the temporal and spatial development of colonization. Water contents and hydraulic flow paths were determined by measuring the transmission of light through the system.

Bacterial growth and accumulation over the one-week course of the experiment had a significant impact on the hydraulic properties of the otherwise homogeneous media. Microbial colonization caused localized drying within the colonized zone with decreases in saturation approaching 50%, and a 5 cm lowering of the capillary fringe height. Flow was retarded within the colonized zone and diverted around it. The apparent solute velocity through the colonized region was reduced from 0.39 cm min^{-1} ($R^2 = 0.99$) to 0.25 cm min^{-1} ($R^2 = 0.99$) by the sixth day of the experiment. In turn, diverted flow probably contributed to large changes observed in the extent of colonization over the course of the experiment. We also observed bacterial migration upward against flow. We hypothesize that the distribution of cells was not determined by water flow alone, but rather by a dynamic interaction between water flow and microbial growth.

INTRODUCTION

The transport and growth of bacteria in subsurface environments is of great interest in the field of environmental protection. Microorganisms may significantly influence the fate and transport of many contaminants in the vadose zone, either directly, by utilization of contaminants as metabolic or co-metabolic substrates, or indirectly, through microbial-induced modifications of their environment such as alterations in porosity, surface characteristics, pH, and redox (U. S. Dept. of Energy, 2000). Many researchers have studied interactions of biology and hydrology in porous media under saturated flowing conditions. For example, saturated hydraulic conductivity is often reduced by several orders of magnitude because of biomass accumulation over time frames of days to weeks (Oberdorfer and Peterson, 1985; Seki et al., 1998; Taylor and Jaffe, 1990; Vandevivere, 1995; Vandevivere and Baveye, 1992a, 1992b, 1992c; Wu et al., 1997). In unsaturated systems, several studies have addressed the transport of bacteria (Jewett et al., 1999; Powelson and Mills, 1998; Schafer et al., 1998; Tan et al., 1992; Wan et al., 1994), and the biodegradation of model contaminants by bacteria (Allen-King et al., 1996; Estrella et al., 1993; Langner et al., 1998), but studies addressing the impact of microbial growth on the hydrologic properties of unsaturated porous media are lacking (Rockhold et al., 2001).

It would be useful to be able to make real time measurements to determine how environmental stimuli such as water flow and nutrient transport spatially impact microbial growth under unsaturated flow conditions, and, in turn, how

microbial growth subsequently impacts water flow and solute transport. Work in our lab has been directed toward the development of a novel method that allows direct, continuous observation of microbial distribution and activity as well as water content and solute transport in unsaturated porous media. This method merges two recently developed technologies: (1) the use of light transmission chambers to quantify pore water content and hydraulic flow paths (Glass et al., 1989; Tidwell and Glass, 1994; Niemet and Selker, 2001; Chapter 2) and (2) the use of bioluminescent bacteria to monitor microbial growth and activity noninvasively in these chambers (Chapters 2 and 3).

Recent work demonstrated the ability to utilize the salicylate-inducible bioluminescence of *Pseudomonas fluorescens* HK44 to quantify its population density in unsaturated sands (Uesugi, et al., in review) and resulted in the development of a model describing the cell-density-dependent bioluminescence response of *P. fluorescens* HK44 that was applied to the use of bioluminescence to measure population densities under unsaturated flowing conditions (Chapter 3).

The objective of the work presented in this chapter was to use light transmission techniques to noninvasively monitor in real-time the impact of microbial growth on water flow and solute transport in unsaturated porous media.

MATERIALS AND METHODS

Chamber, associated equipment, bacterial strain, and growth conditions

Details of the light transmission chamber (Fig. 4.1), light detection system

(CCD camera, lens, and filtration), and fluid application system are described elsewhere (Chapters 2 and 3). The porous medium used in this experiment was 40/50-mesh silica sand, prepared as described previously (Chapter 2). The strain used in this work was *Pseudomonas fluorescens* HK44, supplied by Gary Sayler, University of Tennessee, Knoxville, TN. All liquid media were supplemented with 15 mg L^{-1} tetracycline (Tet15). The basal medium used in the experiment was a nitrate-free minimal mineral salts (MMS) (Chapter 2). Glucose at 250 mg L^{-1} (Glu250), applied through the central dripper only (see Chapter 3), served as the growth substrate. Salicylate, at 100 mg L^{-1} (Sal100), was used to induce the bioluminescent response (see Chapter 3). Chamber preparation, packing, and inoculation were carried out as described previously (Chapters 2 and 3). The porosity of the sand pack was calculated to be 0.332, and the bulk density 1.78 g cm^{-3}. The flow rate per individual dripper was 28.69 ± 0.42 mL h^{-1}, giving an overall flow rate of 315.6 ± 4.6 mL h^{-1}.

Data collection and analytical methods

Water saturation. Transmission images of the chamber were made several times each day (Chapter 2) and water content of the porous media determined by the method of Niemet and Selker (2001).

Flow paths. Flow paths were determined once each day. The central feed dripper was switched over to a solution of MMS+Tet15+Glu250 supplemented with 0.01% (w/v) bromophenol blue dye. After about 20 minutes, the central dripper was switched back to MMS+Tet15+Glu250. The progress of the dye

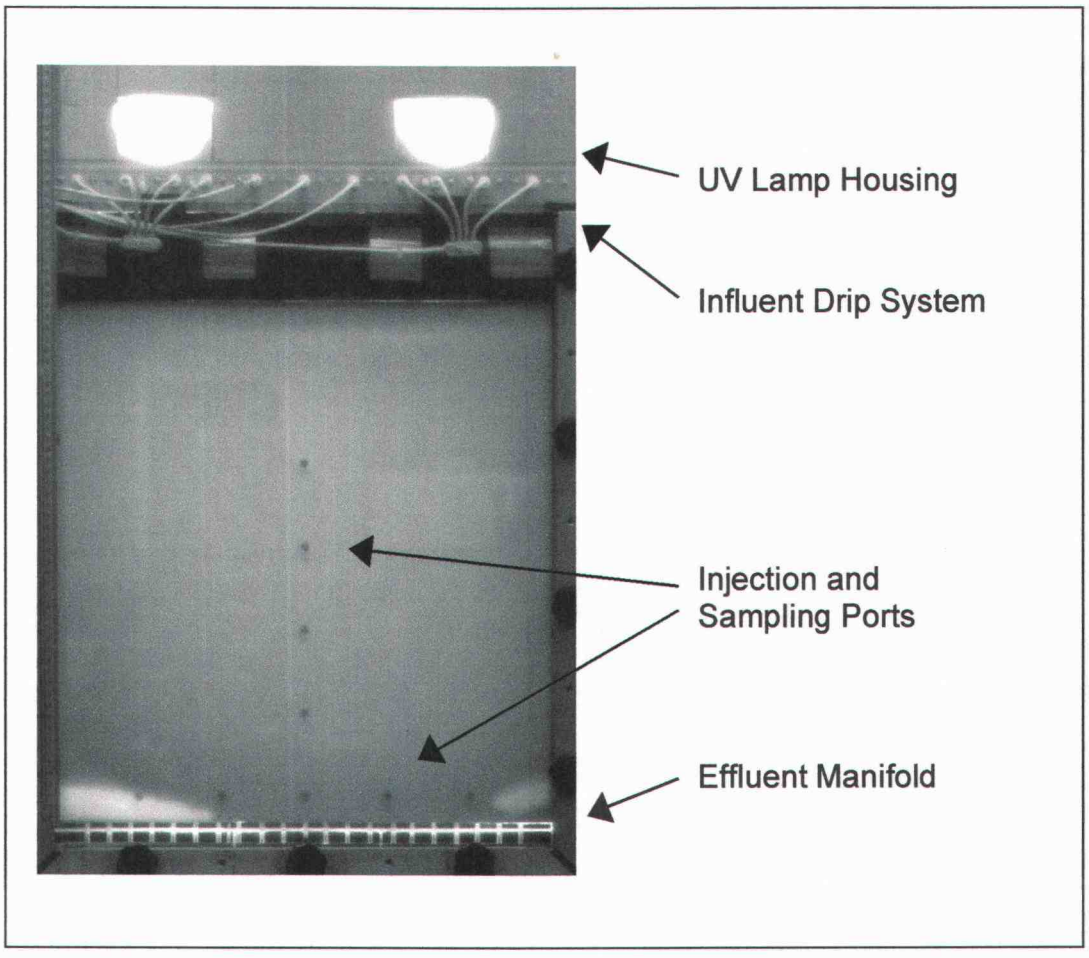

Figure 4.1. Photograph of light transmission chamber.

plume through the chamber was recorded with a series of transmission images at timed intervals. Imaging was continued until the dye plume cleared the chamber.

Bioluminescence. The salicylate-inducible bioluminescence response of *P. fluorescens* HK44 was measured daily, as described in Chapter 3.

Image analysis. Digital image processing was performed using Transform 3.4 (Fortner Software LLC, Sterling, VA) as described in Chapter 2.

Effluent sampling. Chamber effluent was analyzed for microbial biomass and glucose concentrations as described previously (Chapter 3).

Final destructive sampling of the sand. At the end of the experiment, the chamber contents were destructively sampled and analyzed for biomass, total neutral polysaccharide, and gravimetric water content distributions. The sampling method was described in Chapters 2 and 3. Sand samples were extracted with MMS to remove cells. Biomass was quantified in dilutions of the sand extracts both by viable plate counts on half-strength TSB agar supplemented with tetracycline and by total protein analysis. For gravimetric analysis, samples were oven dried at 50°C to constant weight. Total neutral polysaccharide was determined on the same samples previously used for gravimetric analysis. Cell protein was measured using bicinchoninic acid (BCA) (Smith et al., 1985) with the Micro BCA Protein Assay Reagent Kit (Pierce, Rockford, IL), and total neutral polysaccharide in the sand was determined using anthrone (Brink et al., 1960).

Surface tension measurements. Air-liquid interfacial tensions were measured using a DuNoüy ring-tensiometer (CSC Scientific Co., Fairfax, VA). A

platinum ring of known circumference was submersed in the liquid and then slowly raised through the interface. The interfacial tension was determined from the force applied on the ring at the instant that the interfacial surface was broken. Measurements were made on influent solutions, deionized water, and chamber effluent samples, and also on *P. fluorescens* HK44 cell suspensions. Influent and effluent samples were obtained during a second chamber experiment run under the same conditions as the experiment presented here. A similar lowering of the capillary fringe and drying behavior in the colonized region was noted in that experiment (data not shown). For measurements on cell suspensions, *P. fluorescens* HK44 was grown overnight in MMS supplemented with 1 g L^{-1} glucose. The overnight culture was either serially diluted into MMS, or the cells were pelleted by centrifugation, washed, then resuspended and diluted in MMS. In the first case, the samples contained a portion of the spent growth medium along with cells, while in the latter case the samples included cells only. Cell densities were determined from plate counts.

Soil-moisture retention measurements. Water release curves were determined for both clean and colonized 40/50-mesh sand using Tempe cells (Soil Measurement Systems, Tucson, AZ) with hanging water columns. Clean sand was rinsed with distilled water and oven dried before use. The cell density of biomass colonized sand, measured by plate count, was 1.2×10^9 CFU g dry $sand^{-1}$ (equivalent to 0.32 mg dry cells g dry $sand^{-1}$). The colonized sand was gently dried at 50° C and homogenized before use. After packing, the sands were saturated with

distilled water through the hanging column. Different water potential values were then imposed by incremental lowering of the column outlet, and the mass of drained water was measured for each potential value.

RESULTS

Development of colonization

The spatial and temporal development of colonization was monitored by imaging *P. fluorescens* HK44 bioluminescence in response to daily additions of salicylate. Figure 4.2 shows the spatial extent of the colonized region and the model-predicted population density (CFU g dry sand^{-1}) from day 2 to day 7 of the experiment.

Impact of growth on hydraulic properties

Water content distribution. Figure 4.3 shows the pseudo-colorized images of the water saturation distributions in the chamber for day 2 through day 7. The scale on the color bar indicates the level of saturation, with a value of one being fully saturated. Although the vertical banding that appears in the upper, unsaturated, portion of the chamber implies lower water content of the sand, it is not due to microbial growth. The effect was immediately apparent upon initial drainage of the chamber, and did not change over the duration of the experiment. It was likely due to hysteresis in the water retention characteristics of the porous medium that resulted from draining the initially saturated chamber at a faster rate

Figure 4.2. Development of colonization. Images have been colorized to show differences in bioluminescence-predicted population densities for day 2 through day 7. The cross superimposed on the images indicates the inoculation point.

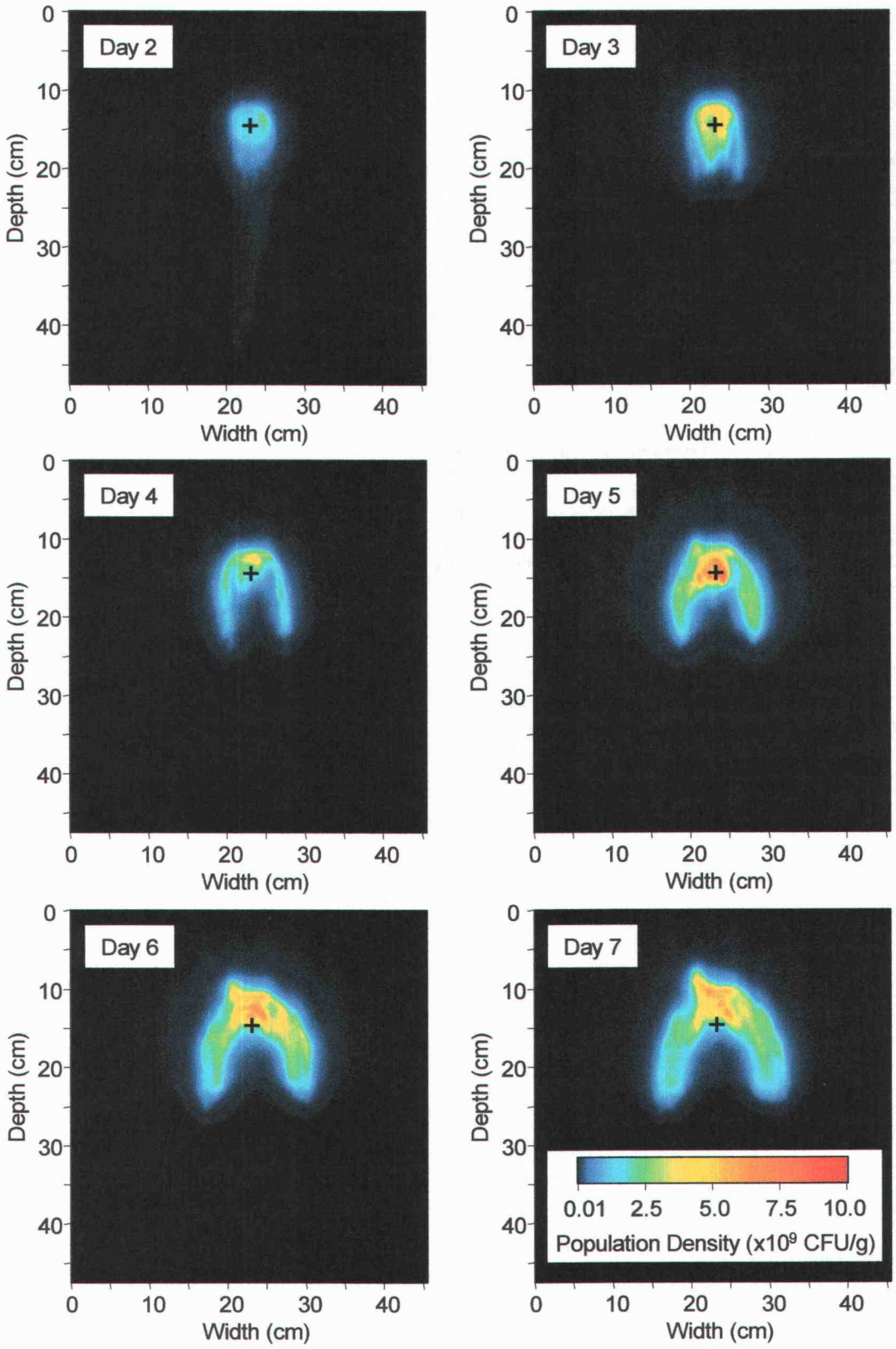
Day 2
Day 3
Day 4
Day 5
Day 6
Day 7
Depth (cm)
Width (cm)
0
10
20
30
40
0.01
2.5
5.0
7.5
10.0
Population Density (x10⁹ CFU/g)

Figure 4.2.

Figure 4.3. Water content distribution. Water content as determined by the light transmission method for day 2 through day 7. The scale indicates level of saturation, with a value of one being fully saturated. The cross on each image indicates the inoculation point.

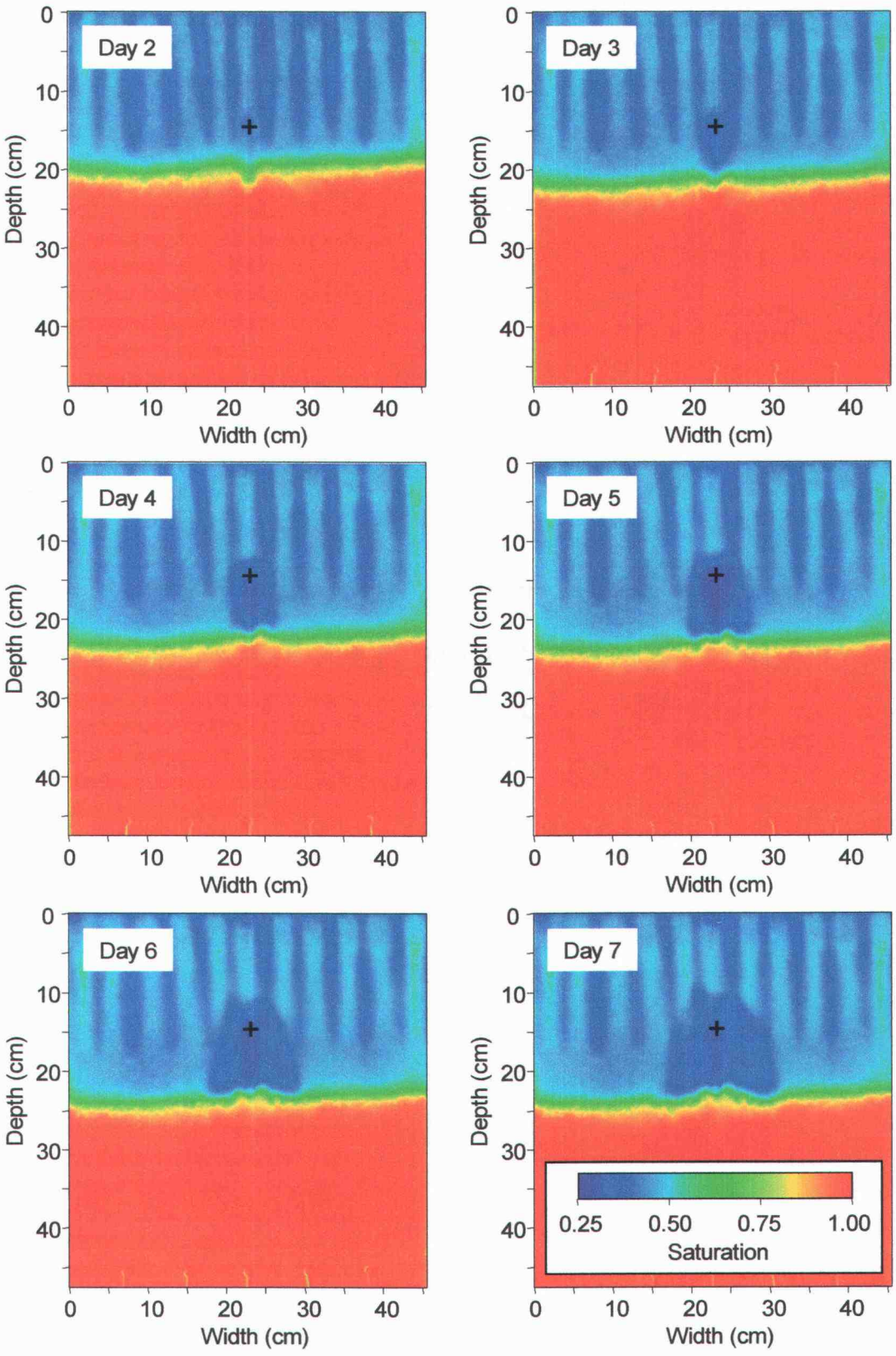
Day 2
Day 3
Day 4
Day 5
Day 6
Day 7
Depth (cm)
Width (cm)
0
10
20
30
40
0.25
0.50
0.75
1.00
Saturation

Figure 4.3.

than the infiltration rate at the upper surface of the chamber. Two noteworthy observations of hydraulic property changes in association with microbial growth are shown. Over the time course of the experiment, the height of the capillary fringe dropped by about 5 cm, and a localized zone of desaturation developed in the vicinity of the colony. Note that the shape of the desaturated zone corresponds with the pattern of bioluminescence shown in Fig. 4.2.

Figure 4.4 shows the change in daily average water contents for a vertical transect of 2.5 cm by 2.5 cm sectors along the midline of the chamber through the colonized region. The midpoint depth for each sector is given in the legend. The colonized region extends from a depth of about 9 cm to a depth of about 26 cm. There was little change in the water content in the sectors above (5, 8.75, and 11.25 cm) or below (26.25 cm and greater) the colony. On the other hand, large changes occurred in the water content within the colony, ranging from 10% to over 50% (depth, change; 13.75, 10%; 16.25, 20%; 18.75, 42%; 21.25, 54%; 23.75, 27%). Water contents were also determined on sand samples by gravimetric analysis at the conclusion of the experiment and compared to water content measured by light transmission immediately prior to the end of the experiment. The mean difference in volumetric water content measured by the two methods was only 0.013 (95% CI 0.0093 to 0.016) for 38 samples from the colonized region (data not shown). This good agreement supports the use of the light transmission method to quantify changes in water saturation in this system even with the presence of high cell densities in the sand.

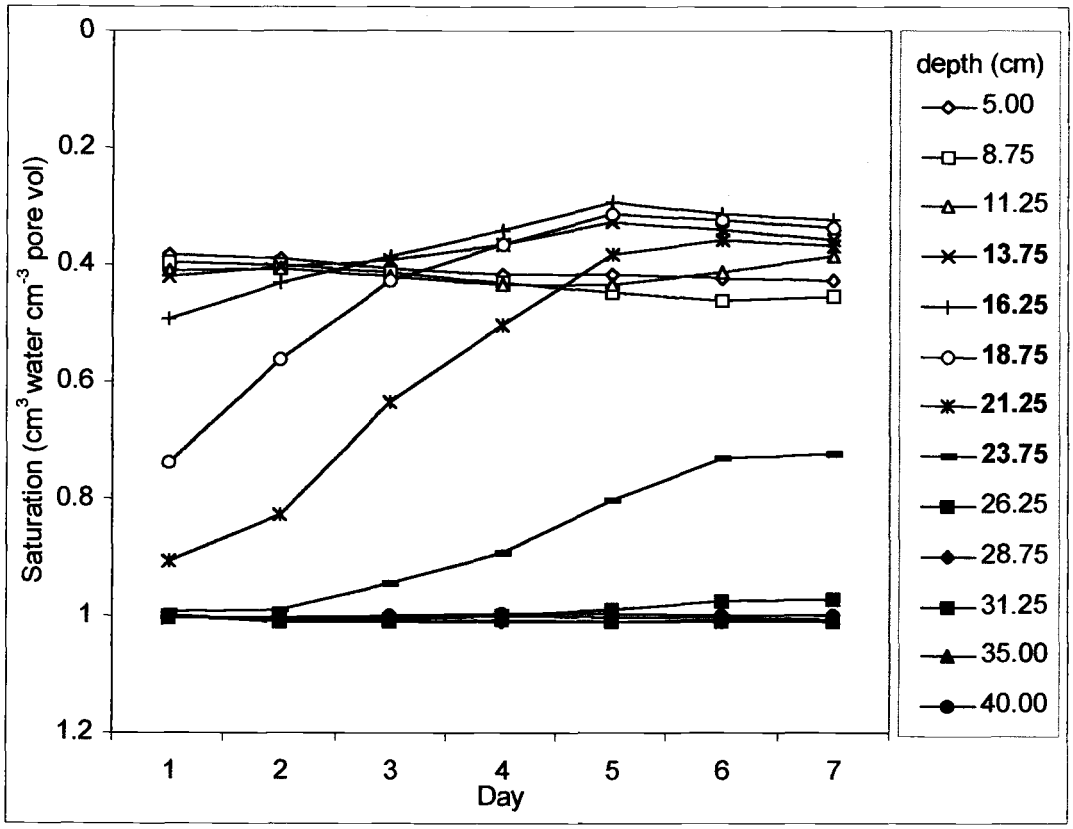

Figure 4.4. Change in water content with time. Averaged saturation levels are shown for a vertical transect of 2.5 cm by 2.5 cm sectors along the midpoint of the chamber. The legend indicates the depth at the midpoint of each sector. Bold figures in the legend indicate samples from within the colonized zone.

Flow paths. The impact of biomass accumulation on the hydraulic and transport properties of the porous medium was evaluated by the periodic addition of a 0.01% (w/v) bromophenol blue dye solution through the center dripper. Figure 4.5 shows the relative attenuation of light transmission (compared to a control image without dye) on a pseudo-colorized scale for day 1 through day 6. The six panels show the position and shape of the dye plume on each day at the same time relative to the start of the dye pulse (about 30 minutes). By day 3, the permeability of the colonized area was reduced enough to distinctly alter the flow of the dye plume relative to that observed one day after the inoculation.

First and second spatial moments. The first and second spatial moments of the dye plumes as a function of time were computed using the method described in Rockhold et al. (1996), as follows:

$$M_x = \frac{1}{M_0} \sum_{i=1}^{n} x_i A_i \qquad (1)$$

$$M_z = \frac{1}{M_0} \sum_{i=1}^{n} z_i A_i \qquad (2)$$

$$M_{xx} = \frac{1}{M_0} \sum_{i=1}^{n} x_i^2 A_i - M_x^2 \qquad (3)$$

$$M_{zz} = \frac{1}{M_0} \sum_{i=1}^{n} z_i^2 A_i - M_z^2 \qquad (4)$$

where

$$M_0 = \sum_{i=1}^{n} A_i \qquad (5)$$

Figure 4.5. Solute flow paths. The scale indicates the relative attenuation of transmitted light compared to an image without dye taken immediately prior to dye application. Images show the position and shape of the dye plumes at the same time relative to the start of each pulse.

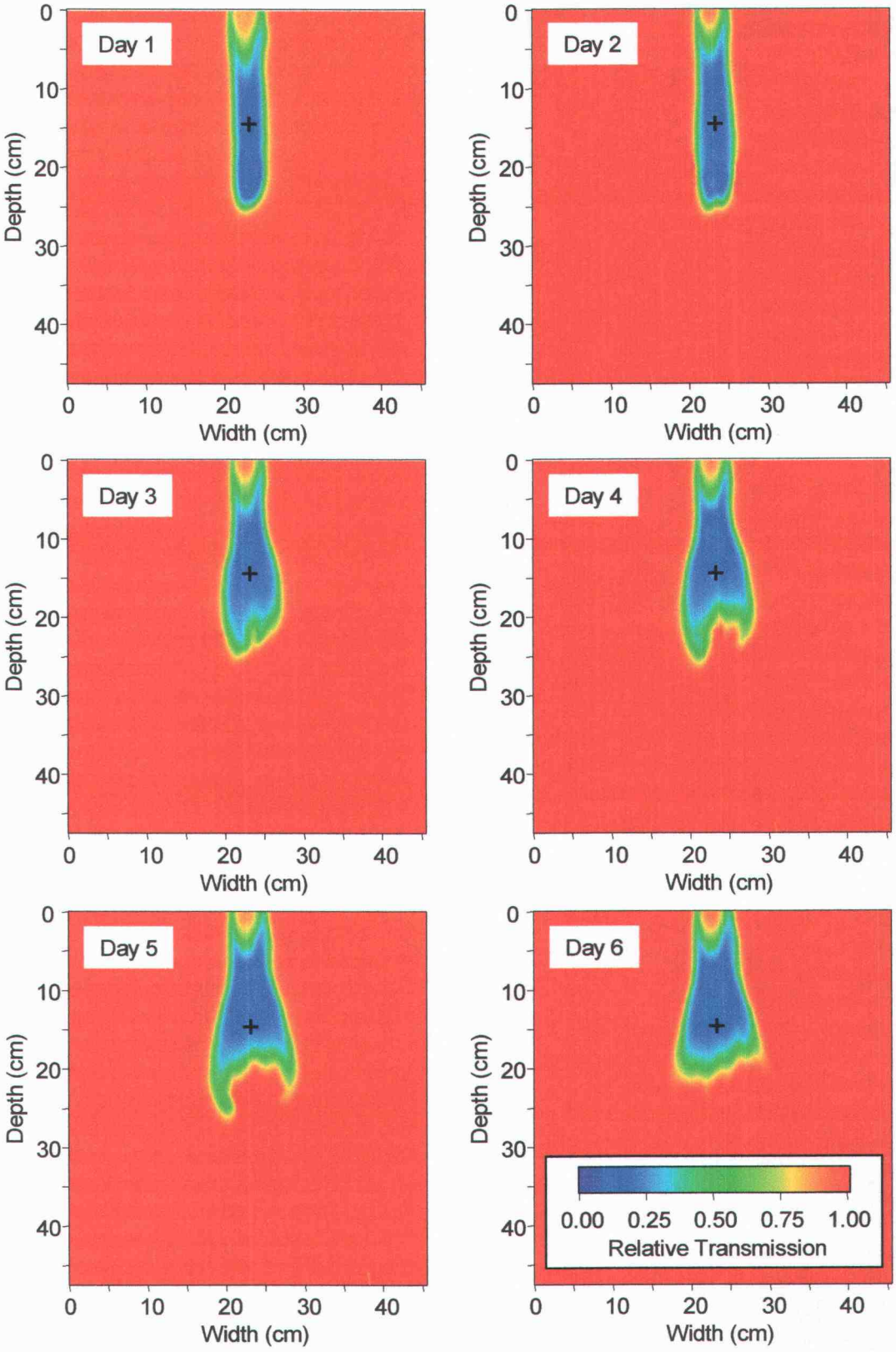
Day 1
Day 2
Day 3
Day 4
Day 5
Day 6
Depth (cm)
Width (cm)
0
10
20
30
40
0.00
0.25
0.50
0.75
1.00
Relative Transmission

Figure 4.5.

and A_i represents the relative attenuation of transmitted light due to the presence of dye at location *i*. The first spatial moments (*Mx, Mz*) represent the location of the center of mass of the plume in the *x* (horizontal) and *z* (vertical) directions, and the second spatial moments (*Mxx, Mzz*) represent the spread of the plume about its center of mass. The values $Mx = 0$ and $Mz = 0$ represent the horizontal midpoint of the chamber and the upper surface of the sand respectively. Summing of the light transmission data across the experimental domain for each series of dye images (for images in which the entire dye plume was within the chamber) revealed that mass was conserved (data not shown), showing that relative attenuation of light can be used as a surrogate for dye concentration. Graphical representations of the results are presented in Fig. 4.6. Data are shown for the first 90 min of each dye pulse, except in the case of the first pulse when data collection stopped after 75 min due to equipment malfunction. The results show a reduction in the effective solute velocity (obstruction effect) through the center of the colonized region (M_z). Regression analysis revealed that on day 1, the apparent solute velocity through the colonized region was 0.39 cm min^{-1} ($R^2 = 0.99$), but by day 6 the apparent velocity was reduced to 0.25 cm min^{-1} ($R^2 = 0.99$). The horizontal dispersion (M_{xx}) of the plume increased, and the vertical dispersion (M_{zz}) of the plume decreased in association with microbial growth over the course of the experiment.

Total neutral polysaccharide and biomass

At the end of the experiment, the chamber contents were destructively sampled and analyzed for biomass protein, total neutral polysaccharide, and

Figure 4.6. First and second spatial moments of the dye plumes. Mx and Mz represent the location of the center of mass in the horizontal and vertical direction respectively, while Mxx and Mzz represent the spread of the plume about its center of mass. Mx = 0, horizontal midpoint of chamber; Mz = 0, upper surface of the sand.

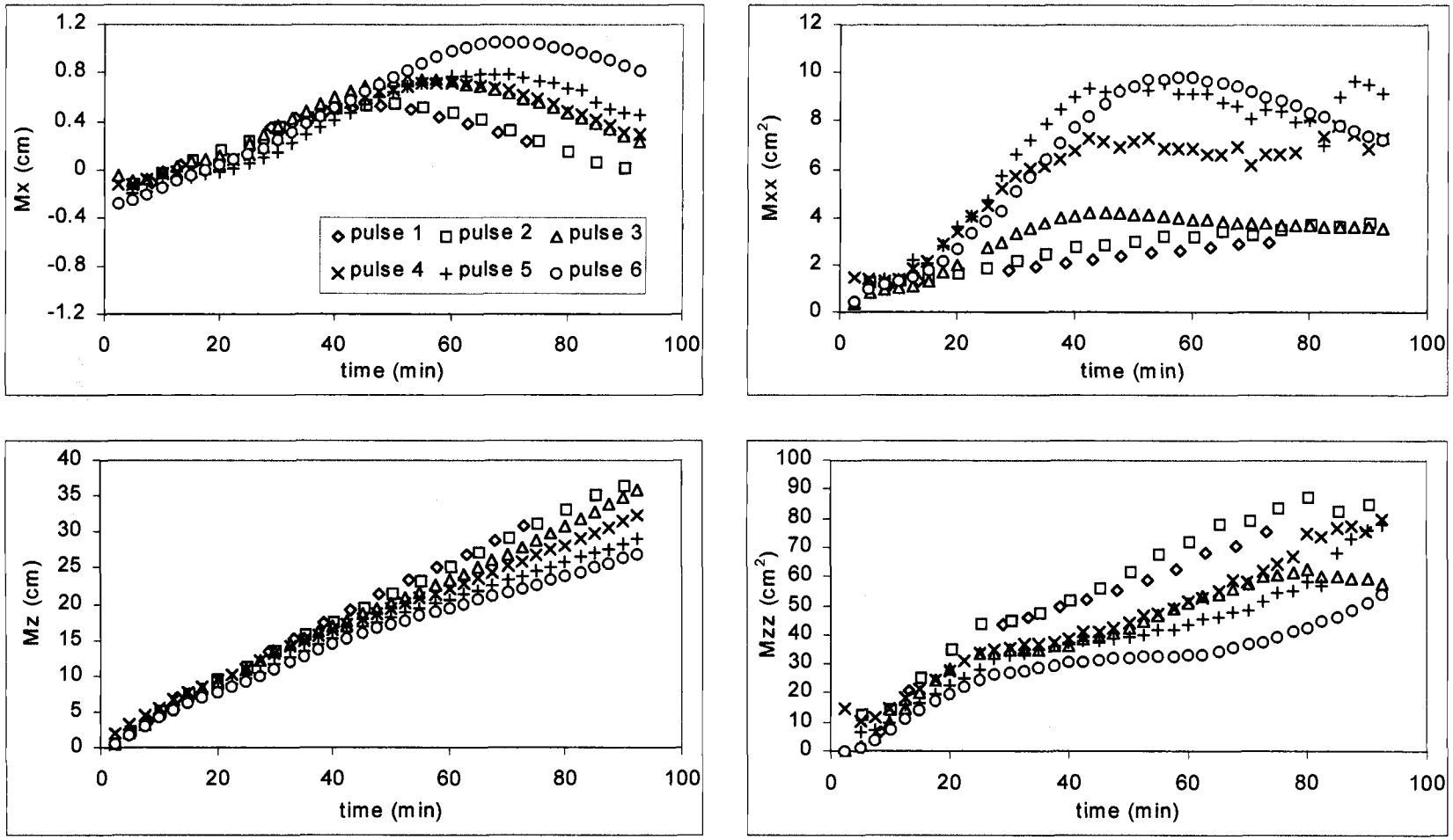
Mx (cm)
time (min)
pulse 1
pulse 2
pulse 3
pulse 4
pulse 5
pulse 6
Mxx (cm²)
time (min)
Mz (cm)
time (min)
Mzz (cm²)
time (min)

Figure 4.6.

gravimetric water content distributions (Table 4.1). Neutral polysaccharide was strongly correlated with protein (r = 0.96), but the ratio of neutral polysaccharide to protein was not correlated with depth or with moisture content. The mean of the ratio was 0.36 (95%CI 0.26 to 0.45). The minimum and maximum ratios were 0.060 and 0.73 respectively.

Sand-moisture retention

Water release curves. Water-release curves were determined for both clean and biomass-affected 40/50 sand using Tempe cells and hanging water columns. The biomass-affected sand showed considerable change in water retention, with air entry occurring by –15 cm in the inoculated material, while requiring –22 cm tension in the pristine media (data not shown).

Surface tension. Air-liquid interfacial tensions were measured on distilled water, influent solutions, chamber effluent samples, and also on *P. fluorescens* HK44 cell suspensions. No significant differences were found between the surface tensions of chamber effluent compared to influent solutions or water (data not shown). No trends were observed for measurements made on MMS suspensions of washed cells. There was a trend observed for a lowering of the surface tensions of *P. fluorescens* HK44 cell suspensions in increasing proportions of spent growth medium. However the magnitude of the differences was less than 1 dyne cm^{-1} over a three-order of magnitude increase in cell concentration, and they did not differ appreciably from the MMS control.

Table 4.1. Polysaccharide and biomass protein in sand samples.

Depth[a] (cm)	Vol. water[b] ($cm^3\ cm^{-3}$)	Polysaccharide[c] ($mg\ kg^{-1}$)	Protein[d] ($mg\ kg^{-1}$)	Ratio ($mg\ mg^{-1}$)
8.75	0.10	3.3	5.1	0.64
8.75	0.12	5.3	62.6	0.08
8.75	0.11	15.5	128.5	0.12
8.75	0.12	3.2	53.3	0.06
8.75	0.13	2.1	3.1	0.67
11.25	0.12	2.9	12.8	0.22
11.25	0.12	20.6	198.1	0.10
11.25	0.09	95.7	424.4	0.23
11.25	0.09	105.4	447.2	0.24
11.25	0.12	20.4	38.4	0.53
11.25	0.12	0.6	1.5	0.37
13.75	0.10	310.2	840.7	0.37
13.75	0.11	177.6	426.2	0.42
13.75	0.14	3.2	4.5	0.71
16.25	0.09	45.3	122.3	0.37
18.75	0.09	55.3	162.0	0.34
18.75	0.13	6.1	8.4	0.73
21.25	0.11	37.7	65.2	0.58
21.25	0.14	3.3	50.6	0.07
23.75	0.20	23.4	63.9	0.37
23.75	0.14	24.4	33.9	0.72
26.25	0.31	14.3	58.9	0.24
28.75	0.32	21.7	113.6	0.19
31.25	0.30	12.7	70.9	0.18

Correlations

	Polysaccharide	Protein	Ratio	Depth
Polysaccharide	1.00			
Protein	0.96	1.00		
Ratio	-0.01	-0.19	1.00	
Depth	-0.09	-0.15	0.01	1.00
Vol. water	-0.25	-0.26	-0.19	0.78

a. depth at midpoint of sample; *b.* volumetric water by gravimetric analysis
c. mg glucose equivalents per kg dry sand; *d.* mg BSA equivalents per kg dry sand

DISCUSSION

Impact of growth on hydraulic properties

Bacterial growth and accumulation had a significant impact on the water retention of unsaturated homogeneous porous media. Microbial colonization caused apparent drying within the colonized zone with localized decreases in saturation approaching 50%, giving rise to diversion of flow around the colonized zone, and a lowering of the capillary fringe.

One might wonder if the drying observed in the colonized region was an artifact of attenuation of the transmitted light by the cells. However, other experiments have shown that cell solutions of 10^9 CFU mL^{-1} had no significant impact on predicted moisture content as determined by the light transmission method under unsaturated or saturated flowing conditions. Furthermore, water contents determined by the gravimetric method upon destructive sampling of colonized sand were in close agreement with those determined by the light transmission method despite cell densities approaching 10^{11} CFU mL^{-1} of pore water (Chapter 2).

Generally, changes in the hydraulic properties of unsaturated porous media due to microbial growth may be a result of physical clogging due to accumulation of cells (Baveye and Valocchi, 1989; Taylor and Jaffe, 1990; Vandevivere, 1995;Vandevivere and Baveye, 1992b, 1992c; Wu et al., 1997), production of extracellular polymers (e.g. Vandevivere and Baveye, 1992a), microbially-generated gases (Oberdorfer and Peterson, 1985; Seki et al., 1998), or

the result of microbially-induced changes in the chemical properties of the liquid or solid phases of the media (Rockhold et al., 2001).

Physical clogging due to microbial growth. Two conceptualizations of the pore-scale pattern of bacterial growth and accumulation that leads to clogging of porous media are represented in the literature (Baveye and Valocchi, 1989). In the first, bacteria are thought to accumulate in a continuous biofilm that uniformly coats the pore walls (e.g. Taylor and Jaffe, 1990). In the second, bacteria are thought to accumulate as discrete microcolonies that may block pore constrictions (e.g. Vandevivere and Baveye, 1992c).

Microscopic observation of *P. fluorescens* HK44 liquid cultures revealed that on average a cell was about 0.8 μm diameter by 2.4 μm long (data not shown). Employing a conservative estimate of 1 μm by 3 μm, a cell occupies a volume of about 2×10^{-12} cm^3 (excluding capsule effects). Given a porosity of 0.332 and bulk density of 1.78, each gram of sand contained 0.19 cm^3 of pore space, so an estimated 1×10^{11} cells g dry $sand^{-1}$ would be required to completely fill the pore volume. The highest cell density measured in this experiment was 6.1×10^9 cells g dry $sand^{-1}$, which would occupy less than 7 % of the available pore space. If a uniform biofilm is assumed, it seems unlikely that space-filling by cells alone could cause the hydraulic changes we observed. However, if the distribution of cells within the sampled volume was highly skewed, it is possible that some proportion of pores could have been completely filled. In sand-column experiments with *Arthrobacter* sp., Vandevivere and Baveye (1992c) used electron microscopy to

show that *Arthrobacter* formed large discontinuous aggregates of cells within the pore spaces that contacted the solid surfaces only at a few points. Three- to four-order of magnitude decreases in saturated hydraulic conductivity were attributed to the blocking of pore necks by cell aggregates. Interestingly, the volume of cells associated with these decreases in conductivity was equivalent to only about 7% of the available pore space (Vandevivere and Baveye, 1992a), which is similar to our observation.

Production of capsule. Soil microbes are often surrounded by a layer of extracellular polysaccharides (EPS) (e.g. Chenu, 1995), and bacterially produced exopolymers can obstruct water flow in porous media. For example, Vandevivere and Baveye (1992a) found that under conditions where cell densities were too low to obstruct water flow, the extracellular polysaccharide had a large impact on saturated conductivity.

There was no evidence that *P. fluorescens* HK44 produced large quantities of EPS under the conditions of this experiment. The maximum ratio of neutral polysaccharide to cell protein (for *P. fluorescens* HK44, protein is 55% of cell dry weight-data not shown) was 0.73 (mg mg^{-1}). The mean ratio was 0.36 (SD 0.22). In contrast, Vandevivere and Kirchman (1993) observed ratios of 4.6 ±0.9 for EPS-producing cells growing in a sand matrix.

Production of gas. Seki et al. (1998) observed that methane produced by bacteria growing on glucose in a saturated flowing system contributed significantly to a reduction of hydraulic conductivity. Similar observations were reported for

production of gases by denitrifiers (Oberdorfer and Peterson, 1985). These gases, produced as byproducts of fermentation and anaerobic respiration, are poorly water-soluble. Because *Pseudomonas fluorescens* HK44 is capable of denitrification (data not shown), we used nitrate-free media so that only aerobic growth would occur. Carbon dioxide, a byproduct of aerobic respiration, is relatively soluble in water. Furthermore, in the unsaturated system described here, assuming a continuous gas path to the atmosphere, gas production should not impact conductivity. We did not observe gas bubbles within the sand nor in the effluent, and it does not seem likely that gas-occlusion factored significantly in the changes in hydraulic properties that we observed.

Microbially induced changes in surface tension. Decreases in liquid retention as a result of microbial colonization are consistent with the observed lowering of the capillary fringe and with the reduction of air-entry pressure. Diversion of flow could be seen as being consistent either with pore clogging and/or with a decrease in unsaturated conductivity due to drying.

The strength with which soil moisture is held by the soil matrix under unsaturated conditions is characterized by the matric potential, or pressure head. The pressure head at which a pore will desaturate is related to the forces of surface tension, as shown by Laplace's equation that describes the height of rise of liquid in a capillary above a free liquid surface,

$$h_d = \frac{2\sigma \cos\gamma}{\rho g r} \qquad (6)$$

where h_d is the pressure head of desaturation, σ is the air-liquid interfacial tension,

γ is solid-liquid contact angle, ρ is the liquid density, g is the gravitational constant, and r is the effective radius of the capillary (soil pore). Soil water content and pore pressure are functionally related, but the relationship is hysteretic, and conductivity is a function of water content. It can be seen by inspection of equation (6) that for a given size pore, changes in surface tension or in contact angle will cause a change in h_d. Local changes in the pressure head alter the hydraulic gradients in a porous media system, changing the magnitude and direction of the driving force for movement of water. Lowering of the surface tension can lead to lower water contents for a given value of pressure head, and in turn lead to a decrease in unsaturated conductivity.

A large volume of literature deals with microbially-produced surface-active compounds (e.g. review by Neu, 1996). Microorganisms may excrete fatty acids, lipids and low molecular weight surfactants such as glycolipids and peptolipids into their surroundings that have the potential to change the air-liquid interfacial tensions or to modify the solid-liquid contact angle. Bacterial cells themselves, by virtue of their surface characteristics, might also modify either of these parameters. Our experiments did not reveal any significant differences between the surface tensions of chamber effluent samples over the time course of the experiment. There was an apparent trend for cell suspensions containing a portion of spent growth media, where surface tensions decreased with increasing concentration of cells (and spent media). However, the magnitude of the differences was slight, and the highest concentration of cells only reduced the surface tension by

approximately one dyne cm^{-1}. This is about an order of magnitude less than would be required to cause the 5 cm lowering of the capillary fringe that we observed. At its greatest extent, however, the colonized region represented only about 10% of the total experimental volume. Any surface-active compounds released into the media would be significantly diluted by mixing with flow from the uncolonized portion of the chamber by the time they reached the effluent. Moreover, if such compounds were produced but became sorbed to the sand or to air-water interfaces, effluent concentrations could be even lower.

Coating of the sand grains with cells might render them more hydrophobic relative to uncoated sand. In our experiments, air entry occurred in colonized sand at a reduced suction compared with the untreated sand, indicating that biomass-affected sand held water less tightly than clean sand.

Development of colonization

Dramatic changes in the extent of colonization occurred over the course of the experiment, including definite upward migration against flow. This is particularly interesting because the upward migration against flow cannot be explained by passive transport. *P. fluorescens* is a motile organism, and the observed migration against flow may have been a response to the gradient in glucose and oxygen. Lawrence et al. (1987) observed similar behavior for *P. fluorescens* colonization in flow cells. We hypothesize that the distribution of cells was not determined only by water flow, but rather by a dynamic interaction between flow and microbial growth. As cell densities increased, water flow and

solute transport through the colonized region was retarded and redirected laterally around it. Cells that detached from the upper reaches of the colonized zone may have been transported by this diverted flow to reattach and grow elsewhere. Much of the lateral increase in the colonized region can be explained by such a process of redistribution with the water flow. Alternatively it may be postulated that the lateral spread of colonization was driven by movement of *P. fluorescens* HK44 in response to gradients in glucose and oxygen that developed as water flow was diverted around the colonized region. The interesting observation in either case was that the change in direction of flow was caused by the activities of the organisms themselves.

It was interesting to find that high numbers of viable cells remained associated with the sand from the interior of the colony where glucose and oxygen presumably were limited. Some researchers have reported that nutrient depletion can lead to deadhesion of attached cells (Allison et al., 1998). The high numbers of cells retained in the interior of the colonized zone may be explained by the desaturation phenomenon that was observed. Over the past decade, researchers have become increasingly aware of the role of air-water interfaces in microbial transport in unsaturated systems (Powelson and Mills, 1996, 1998; Schafer et al., 1998; Wan et al., 1997; Jewett et al., 1999). Bacteria tend to accumulate at air-water interfaces, and the retention of bacteria in porous media is proportional to the fraction of air-occupied pore space. Trapping of bacteria at air-water interfaces is an important process that may control bacterial transport in unsaturated soils. As

the interior of the colonized zone desaturated, more air-liquid interfacial area was created, possibly leading to increased immobilization of cells.

Many interesting questions have been raised that are pertinent to enhancing our understanding of the interactions between microbial growth and hydrology under unsaturated flowing conditions. Refinement of experimental approaches and data collection systems will continue to challenge scientists interested in this area of study.

CHAPTER 5

SUMMARY

There is a good deal of developing interest in the understanding of bacterial behavior in subsurface environments, largely because of the great potential for *in situ* bioremediation of contaminants released into such environments. At present, further refinement of this technology is hindered because of lack of knowledge of the basic characteristics of bacterial growth in unsaturated media (e.g. U. S. Dept. of Energy, 2000). While a number of researchers have studied interactions of bacteria and hydrology in porous media under saturated flowing conditions, and biomass accumulation has been shown to cause significant changes in hydrologic properties such as reductions in saturated hydraulic conductivity (e.g. Taylor and Jaffe, 1990; Vandevivere and Baveye, 1992a, 1992c), studies addressing the impact of bacterial growth on the hydrologic properties of unsaturated porous media are lacking (Rockhold et al., 2001). In this thesis I have described the development of a lab-scale experimental system to examine, noninvasively, interactions between microbial growth, water flow, and solute transport in unsaturated porous media. The system allows direct, continuous observation of bacterial distribution and activity as well as water content distribution and flow paths. This was made possible through CCD imaging of a combination of two recently developed light-based technologies: (1) light transmission chambers to quantify pore water content and hydraulic flow paths (e.g. Niemet and Selker, 2001; Selker, 1991) and (2) a bioluminescent reporter bacterium, *Pseudomonas fluorescens* HK44 (King et al., 1990), to monitor microbial growth and activity in these chambers. The specific objectives of this

work were: (1) to adapt the 2D light transmission chambers to successfully carry out microbiological experiments, (2) to determine whether a model, developed under static conditions, relating *P. fluorescens* HK44 cell density to the rate of increase in light production after induction would successfully quantify growth under unsaturated flowing conditions, (3) to use bioluminescence to noninvasively map the spatial and temporal development of microbial colonization in the 2D chambers under unsaturated flowing conditions, and (4) to simultaneously monitor the impact of microbial colonization on the hydrologic properties of the porous medium using light transmission to measure water contents and solute flow paths.

Several bioengineering problems associated with chamber design and function required solution before microbial experiments were successful. These included: choice of materials for chamber components; development of sterilization, packing, and inoculation protocols; and development of procedures for data collection and chamber maintenance during experiments lasting several days. For example, localized subsurface point inoculation was superior to uniform inoculation of the sand in which case the majority of growth and activity occurred at the surface of the sand rather than within the subsurface. It was also important to determine if bacterial cell suspensions would influence apparent saturation measured by light transmission. The presence of *P. fluorescens* HK44 colonization did not have a significant impact on the ability of the light transmission method to accurately quantify water content distributions in the system. The mean value for the ratio of transmitted light in the presence of 10^9 CFU mL^{-1} to transmitted light in

the absence of cells was 1.001 (SD 0.003) under unsaturated conditions and 0.994 (SD 0.006) under saturated conditions. Water content determined by the light transmission method agreed with water content determined by gravimetric analysis for colonized sands with cell densities ranging from none detected to 9×10^{10} CFU mL^{-1} of pore water. The mean difference in saturation determined by the two methods was 0.050 (95% CI 0.038 to 0.063).

The application of a nonlinear model relating the rate of increase in light-emission after salicylate exposure to microbial density (Uesugi et al., in review) successfully predicted cell densities of *P. fluorescens* HK44 over four orders of magnitude ($R^2 = 0.95$) for colonized regions where oxygen availability and metabolic state were assumed to be non-limiting. Total growth predicted by the model over a seven-day experiment also agreed with potential growth calculated from the mass balance of the system and previously established kinetic parameters (predicted, 1.2×10^{12} cells; calculated, 1.7×10^{12} cells). The predicted and calculated populations in the chamber at the end of the experiment were 6.0×10^{10} cells and 6.1×10^{10} cells, respectively. Other studies have reported a linear relationship between light emission and cell density either when the bioluminescence was measured at a fixed time point after induction or when peak bioluminescence was related to cell concentration (e.g. Neilson et al., 1999; Rattray et al., 1990). Although Neilson et al. (1999) found a strong relationship ($R^2 = 0.997$) between peak bioluminescence and cell density, the time required to reach peak bioluminescence also varied with cell density (between two and eight

hours). In a dynamic system, it is important to quantify density as quickly as possible to avoid complications arising when changes occur in the system (such as in population densities, oxygen levels, and water contents) over shorter timescales than required to obtain the bioluminescence data. The relationship between the rate of increase in light production and cell density permits measurements to be made quickly, because cells need only be exposed to inducer for sufficient time to determine the rate of increase in light emission. Limitations with the model included a tendency to over-predict colonization in sectors just outside the colony due to the lantern effect described in Chapter 3. Light transmitted from colonized regions to uncolonized regions required identification of the spatial extent of colonization by way of a threshold. Moreover, the magnitude of colonization was under-predicted in sectors within and below the colony, apparently due to oxygen limitation. On the other hand, the observation of the development of the dark interior region of the colony points out the potential usefulness of bioluminescence to map the location and spatial and temporal development of aerobic and anaerobic zones in this dynamic experimental system. To further refine the system it would be useful to have a second marker, independent of oxygen or metabolic state, to quantify microbial distribution, while *lux* expression would be employed as an indicator of cell status and oxygen availability. For example, GFP/*lux*-marked organisms would permit independent observation of both microbial distribution and O_2-dependent activity. Preliminary experiments, not shown here, indicate that the

2D light transmission chambers can be modified to enable GFP excitation and detection, and efforts to optimize the system are ongoing.

Bacterial growth and accumulation had a significant impact on the hydrologic properties of the otherwise homogeneous unsaturated porous media. Microbial colonization caused apparent drying within the colonized zone with localized decreases in saturation approaching 50%, giving rise to diversion of flow around the colonized zone, and a lowering of the capillary fringe. Determination of the particular mechanisms that led to the observed changes will require further study. Changes in the hydraulic properties of unsaturated porous media due to microbial growth have been associated with a number of mechanisms, including physical clogging due to accumulation of cells (e.g. Baveye and Valocchi, 1989; Taylor and Jaffe, 1990), production of extracellular polymers (e.g. Vandevivere and Baveye, 1992a), and microbially-induced changes in the chemical properties of the liquid or solid phases of the media (Rockhold et al., 2001). In the experiments described here, the highest measured cell density (6.1×10^9 cells g dry sand^{-1}) would occupy less than 7 % of the available pore space. If a continuous biofilm that uniformly coats pore walls is assumed, as proposed by Taylor and Jaffe (1990), it seems unlikely that space-filling by cells alone could cause the hydraulic changes we observed. However, in saturated sand-column experiments, Vandevivere and Baveye (1992c) found that *Arthrobacter* formed large discontinuous aggregates of cells within the pore spaces that contacted the solid surfaces only at a few points. Three- to four-order of magnitude decreases in saturated hydraulic conductivity

were attributed to the blocking of pore necks by cell aggregates. The volume of cells associated with these decreases in conductivity was equivalent to only about 7% of the available pore space which is similar to the results I have reported here. In other experiments, Vandevivere and Baveye (1992a) found that under conditions where cell densities were too low to obstruct water flow, the extracellular polysaccharide produced by another bacterium had a large impact on saturated conductivity. In the experiments I have described, however, there was no evidence that *P. fluorescens* HK44 produced large quantities of EPS. The maximum ratio of neutral polysaccharide to cell protein was 0.73 (mg mg^{-1}), and the mean ratio was 0.36 (SD 0.22). In contrast, Vandevivere and Kirchman (1993) observed ratios of 4.6 ±0.9 for EPS-producing cells growing in a sand matrix. Finally, coating of the sand grains with cells might render them more hydrophobic relative to uncoated sand. In water-retention experiments using Tempe cells with hanging water columns, air entry in *P. fluorescens* HK44 colonized sand occurred at a reduced suction compared with the untreated sand (15 cm in the inoculated material; –22 cm tension in the pristine media), indicating that biomass-affected sand held water less tightly than clean sand.

Bioluminescence successfully mapped the spatial and temporal development of *P. fluorescens* HK44 colonization under unsaturated flowing conditions. It was interesting to observe the dramatic changes in the extent of colonization that occurred. The distribution of cells was not determined by water flow alone, but rather by a dynamic interaction between flow and microbial growth.

As cell densities increased, water flow and solute transport through the colonized region was retarded and redirected laterally around it. Cells that detached from the upper reaches of the colonized zone may have been transported by this diverted flow to reattach and grow elsewhere. Much of the lateral increase in the colonized region can be explained by such a process of redistribution with the water flow. Alternatively the lateral spread of colonization may have been driven by movement of *P. fluorescens* HK44 in response to gradients in glucose and oxygen that developed as water flow was diverted around the colonized region. It was particularly interesting to observe upward migration against flow, because that cannot be explained by passive transport processes. *P. fluorescens* is a motile organism, and the observed migration against flow may have been a response to the gradient in glucose and oxygen. Lawrence et al. (1987) observed similar behavior for *P. fluorescens* colonization in flow cells. It was also interesting that while the rate of areal expansion of the colonized zone and the predicted populations in the newly colonized regions remained relatively constant, the proportion of daily potential growth that remained within the chamber declined over time. The fact that populations also continued to increase in the "one-day-old" colonized regions indicates that glucose and oxygen delivery to these regions was maintained for some time. Further studies are needed to determine from where within the colonized zone the effluent cells originate; whether they are actively growing cells released into the aqueous phase through the process of cell division, attached cells detached from sand due to shear forces, or less metabolically active cells

originating from interior regions of the colonized zone where nutrients become limited. Others have reported that starvation conditions may stimulate detachment of attached cells (e.g. Allison et al., 1998). It was also intriguing to find that high numbers of viable cells remained associated with the sand from the interior of the colony where glucose and oxygen presumably were limited. The high numbers of cells retained in the interior of the colonized zone may be explained by the desaturation phenomenon that was observed. Bacteria tend to accumulate at air-water interfaces, and the retention of bacteria in porous media is proportional to the fraction of air-occupied pore space (e.g. Powelson and Mills, 1996, 1998; Schafer et al., 1998; Wan et al., 1997; Jewett et al., 1999). As the interior of the colonized zone desaturated, more air-liquid interfacial area was created, which may have led to increased immobilization of cells.

These experiments provided the proof-of-concept for combining light transmission and bioluminescence technologies to study interactions between microbial growth and hydrology in unsaturated porous media. Many interesting observations were made and questions have been raised that are pertinent to enhancing our understanding of the interactions between microbial growth and hydrology under unsaturated flowing conditions. With ongoing refinement, this useful experimental system will continue to provide interesting opportunities to study interactions between microbial dynamics, water flow, and solute transport in unsaturated porous media.

BIBLIOGRAPHY

Allen-King, R. M., R. W. Gillham, J. F. Barker, and E. A. Sudicky. 1996. Fate of dissolved toluene during steady infiltration through unsaturated soil: II. biotransformation under nutrient-limited conditions. J. Environ. Qual. 25: 287-295

Allison, D. G., B. Ruiz, C. SanJose, A. Jaspe, and P. Gilbert. 1998. Extracellular products as mediators of the formation and detachment of *Pseudomonas fluorescens* biofilms. FEMS Microbiol. Lett. 167: 179-184.

Applegate, B. M., S. R. Kehrmeyer, and G. S. Sayler. 1998. A chromosomally based *tod-luxCDABE* whole-cell reporter for benzene, toluene, ethylbenzene, and xylene (BTEX) sensing. Appl. Environ. Microbiol. 64 2730-2735.

Baveye, P., and A. Valocchi. 1989. An evaluation of mathematical models of the transport of biologically reacting solutes in saturated soils and aquifers. Water Resources Research. 25:1413-1421.

Beauchamp, C. J., J. W. Kloepper, and P. A. Lemke. 1993. Luminometric analysis of plant root colonization by bioluminescent pseudomonads. Can. J. Microbiol. 39: 434-441.

Blouin, K., S. G. Walker, J. Smit, and R. F. B. Turner. 1996. Characterization of *in vivo* reporter systems for gene expression and biosensor applications based on *luxAB* luciferase genes. Appl. Environ. Microbiol. 62: 2013-2021.

Bolenes, J., D. Zoutman, J. Campbell, W. Verstraete, and W. Paranchych, 1993. The use of bioluminescence as a reporter to study the adherence of the plant growth promoting rhizopseudomonads 7NSK2 and ANP15 to canola roots. Can. J. Microbiol. 39:329-34.

Brink, R. H., P. Dubach, and D. L. Lynch. 1960. Measurement of carbohydrates in soil hydrolyzates with anthrone. Soil. Sci. 89:157-166.

Burlage, R. S., G. S. Sayler and F. Larimer. 1990. Monitoring of naphthalene catabolism by bioluminescence with *nah-lux* transcriptional fusions. J. Bacteriol. 172: 4749-4757.

Chenu, C. 1995. Extracellular polysaccharides: an interface between microorganisms and soil constituents. pp 217-233. *In* P. M. Huang, J. Berthelin, J. M. Bollag, W. B. McGill and A. L. Page (ed.), Environmental impact of soil components interactions, vol. 1., natural and anthropogenic organics. Lewis, New York.

Craun, G. F. 1985. A summary of waterborne illness transmitted through contaminated groundwater. J. Environ. Health. 48: 122-127.

deWeger L. A., P. Dunbar, W. Mahafee, B. Lugtenberg and G. S. Sayler. 1991. Use of bioluminescence markers to detect *Pseudomonas* spp. in the rhizosphere. Appl. Environ. Microbiol. 57: 3641-3644.

Duncan, S., L. A. Glover, K. Killham, and J. I. Prosser. 1994. Luminescence-based detection of activity of starved and viable but nonculturable bacteria. Appl. Environ. Microbiol. 60: 1308-1316.

Estrella, M. R., M. L. Brusseau, R. S. Maier, I. L. Pepper, P. J. Wierenga and R. M. Miller. 1993. Biodegradation, sorption, and transport of 2,4-D acid in saturated and unsaturated soils. Appl. Environ. Microbiol. 59: 4266-4273.

Flemming, C. A., K. T. Leung, H. Lee, and J. T. Trevors. 1994a. Bioluminescent most-probable-number method to enumerate *lux*-marked *Pseudomonas aeruginosa* UG2Lr in soil. Appl. Environ. Microbiol. 60: 3458-3461.

Flemming, C. A., K. T. Leung, H. Lee, J. T. Trevors, and C. W. Greer. 1994b. Survival of *lux-lac*-marked biosurfactant-producing *Pseudomonas aeruginosa* UG2L in soil monitored by nonselective plating and PCR. Appl. Environ. Microbiol. 60: 1606-1613.

Glass, R. J., T. S. Steenhuis, and J-Y. Parlange. 1989. Mechanism for finger persistence in homogenous unsaturated porous media: Theory and verification. Soil Sci. 148: 60-70.

Hastings, J. W. and K. H. Nealson. 1977. Bacterial bioluminescence. Ann. Rev. Microbiol. 31: 549-595

Heitzer, A., B. M. Applegate, S. R. Kehrmeyer, H. Pinkart, O. F. Webb, T. J. Phelps, D. C. White, and G. S. Sayler. 1998. Physiological considerations of environmental applications of *lux* reporter fusions. J. Microbiol. Methods 33: 45-57.

Heitzer, A., K. Malachowsky, J. E. Thonnard, P. R. Bienkowski, D. C. White, and G. S. Sayler. 1994. Optical biosensor for environmental on-line monitoring of naphthalene and salicylate bioavailability with an immobilized bioluminescent catabolic reporter bacterium. Appl. Environ. Micrbiol. 60: 1487-1494.

Heitzer A., O. F. Webb, J. E. Thonnard and G. S. Sayler. 1992. Specific and quantitative assessment of naphthalene and salicylate bioavailability by using a bioluminescent catabolic reporter bacterium. Appl. Environ. Microbiol. 58: 1839-1846.

Hoa, N. T. 1981. A New Method Allowing the Measurement of Rapid Variations on the Water Content in Sandy Porous Media. Wat. Resour. Res. 17 1: 41-48.

Jewett, D. G., B. E. Logan, R. G. Arnold, and R. C. Bales. 1999. Transport of *Pseudomonas fluorescens* through quartz sand columns as a function of water content. J. Contam. Hydrol. 36: 73-89.

King, J. M. H., P. M. DiGrazia, B. M. Applegate, R. S. Burlage, J. Sanseverino, P. Dunbar, F. Larimer and G. S. Sayler. 1990. Rapid, sensitive bioluminescent reporter technology for naphthalene exposure and biodegradation. Science 249: 778-781.

Langner, H. W., W. P. Inskeep, H. M. Gaber, W. L. Jones, B. S. Das, and J. M Wraith. 1998. Pore water velocity and residence time effects on the degradation of 2,4-D during transport. Environ. Sci. Technol. 32: 1308-1315.

Lawrence, J. R., P. J. Delaquis, D. R. Korber, and D. E. Caldwell. 1987. Behavior of *Pseudomonas fluorescens* within the hydrodynamic boundary layers of surface microenvironments. Microb. Ecol. 14: 1-14.

Lindow, S. E. 1995. The use of reporter genes in the study of microbial ecology. Molec. Ecol. 4: 555-566.

Matrubutham, U., J. E. Thonnard, and G. S. Sayler. 1997. Bioluminescence induction response and survival of the bioreporter bacterium *Pseudomonas fluorescens* HK44 in nutrient-deprived conditions. Appl. Microbiol. Biotechnol. 47: 604-609.

Meighen, E. A. 1988. Enzymes and genes from the *lux* operons of bioluminescent bacteria. Ann. Rev. Microbiol. 42: 151-176.

Meighen, E. A. 1991. Molecular biology of bacterial bioluminescence. Microbiol. Rev. 55: 123-142.

Meighen, E. A. 1993. Bacterial bioluminescence: organization, regulation, and application of the *lux* genes. FASEB J. 7: 1016-1022.

Meighen, E. A., and P. V. Dunlap. 1993. Physiological, biochemical and genetic control of bacterial bioluminescence. Adv. Microb. Physiol. 34: 2-67.

Meikle, A., K. Killham, J. I. Prosser, and L. A. Glover. 1992. Luminometric measurement of population activity of genetically modified *Pseudomonas fluorescens* in the soil. FEMS Microbiol. Lett. 99: 217-220.

Neilson, J. W., S. A. Pierce, and R. M. Maier. 1999. Factors influencing expression of *luxCDABE* and *nah* genes in *Pseudomonas putida* RB1353 (NAH7, pUTK9) in dynamic systems. Appl. Environ. Microbiol. 65: 3473-3482.

Neu, T. R. 1996. Significance of bacterial surface-active compounds in interaction of bacteria with interfaces. Microbiol. Rev. 60:151-166.

Niemet, M. R., and J. S. Selker. 2001. A new method for quantification of liquid saturation in 2-d translucent porous media systems using light transmission. Advan. Water Resour. 24:651-666.

Oberdorfer, J. A., and F. L. Peterson. 1985. Waste-water injection: geochemical and biogeochemical clogging processes. Ground Water. 23: 753-761.

O'Kane, D. J., W. L. Lingle, J. E. Wampler, M. Legocki, R. P. Legocki, and A. A. Szalay. 1988. Visualization of bioluminescence as a marker of gene expression in *Rhizobium*-infected soybean root nodules. Plant Molec. Biol. 10: 387-399.

Powelson. D. K., and A. L. Mills. 1996. Bacterial enrichment at the gas-water interface of a laboratory apparatus. Appl. Environ. Microbiol. 62: 2593-2957.

Powelson. D. K., and A. L. Mills. 1998. Water saturation and surfactant effects on bacterial transport in sand columns. Soil Sci. 163: 694-704.

Rattray, E. A. S., J. I. Prosser, K. Killham, and L. A. Glover. 1990. Luminescence-based nonextractive technique for in situ detection of *Escherichia coli* in soil. Appl. Environ. Microbiol. 56: 3368-3374.

Rockhold, M. L., R. E. Rossi, and R. G. Hills. 1996. Application of similar media scaling and conditional simulation for modeling water flow and tritium transport at the Las Cruces trench site. Wat. Resour. Res. 32:595-609.

Rockhold, M. L., R. R. Yarwood, M. R. Niemet, P. J. Bottomley, and J. S. Selker. 2001. Considerations for modeling bacterial-induced changes in hydraulic properties of variably saturated porous media. Advan. Water Resour. Manuscript in press.

Schafer, A., P. Ustohal, H. Harms, F. Stauffer, T. Dracos, and A. Zehnder. 1998. Transport of bacteria in unsaturated porous media. J. Contam. Hydrol. 33: 149-169.

Schell, M. A. 1990. Regulation of the naphthalene degradation genes of plasmid NAH7: example of a generalized positive control system in *Pseudomonas*

and related bacteria, p. 165-176. *In* S. Silver, A. M. Chakrabarty, B. Iglewski, and S. Kaplan (ed.), *Pseudomonas*: biotransformations, pathogenesis, and evolving biotechnology. American Society for Microbiology, Washington, DC.

Schroth, M. H., S. J. Ahearn, J. S. Selker, and J. D. Istok. 1996. Characterization of Miller-similar silica sands for laboratory hydrologic studies. Soil Sci. Soc. Am. J. 60: 1331-1339.

Schroth, M. H., J. D. Istok, S. J. Ahern, and J. S. Selker. 1995. Geometry and position of light nonaqueous-phase liquid lenses in water-wetted porous media. J. Contam. Hydrol. 19: 269-287.

Schroth, M. H., J. D. Istok, J. S. Selker, M. Oostrom, and M. D. White. 1998. Multifluid flow in bedded porous media: laboratory experiments and numerical simulations. Adv. Wat. Res. 22: 169-183.

Seki, K., T. Miyazaki, and M. Nakano. 1998. Effects of microorganisms on hydraulic conductivity decrease in infiltration. Eur. J. Soil Sci. 49: 231-236

Selifonova, O. V., R. S. Burlage and T. Barkay. 1993. Bioluminescent sensors for detection of bioavailable Hg(II) in the environment. Appl. Environ. Microbiol. 59: 3083-3090.

Selker, J. S. 1991. Unstable wetting in homogeneous soils under continuous infiltration. Ph.D. thesis, Cornell University, Ithaca, NY.

Shaw, J. J., F. Dane, D. Geiger, and J. W. Kloepper. 1992. Use of bioluminescence for detection of genetically-engineered microorganisms released into the environment. Appl. Environ. Microbiol. 58: 267-273.

Shaw, J. J., and C. I. Kado. 1986. Development of a vibrio bioluminescence gene-set to monitor phytopathogenic bacteria during the on-going disease process in a non-disruptive manner. Biotechnol. 4: 560-564.

Shaw, J. J., P. Rogowsky, T. J. Close, and C. I. Kado. 1987. Working with bacterial bioluminescence. Plant Molecular Biology Reporter. 5: 225-236.

Smith, P. K., R. I. Krohn, G. T. Hermanson, A. K. Mallia, F. H. Gartner, M. D. Provenzano, E. K. Fujimoto, N. M. Goeke, B. J. Olson, and D. C. Klenk. 1985. Measurement of protein using bicinchoninic acid. Anal. Biochem. 150:76-85.

Stewart, G. S. A. B. 1990. *In vivo* bioluminescence: new potentials for microbiology. Lett. Appl. Microbiol. 10:2-8.

Stewart, G. S. A. B., and P. Williams. 1992. *lux* genes and the applications of bacterial bioluminescence. J. Gen. Microbiol. 138: 1289-1300.

Sticher, P. M. C. M. Jaspers, K. Stemmler, H. Harms, A. J. B. Zehnder, and J. R. van der Meer. 1997. Development and characterization of a whole-cell bioluminescent sensor for bioavailable middle-chain alkanes in contaminated groundwater samples. Appl. Environ. Microbiol. 63: 4053-4060.

Tan, Y., W. J. Bond, and D. M. Griffin. 1992. Transport of bacteria during unsteady unsaturated soil water flow. Soil Sci. Soc. Am. J. 56: 1331-1340.

Taylor S. W. and P. R. Jaffe. 1990. Biofilm growth and the related changes in the physical properties of a porous medium. Water Resour. Res. 26: 2153-2159.

Tidwell, V. C., and R. J. Glass. 1994. X-ray and visible light transmission for laboratory measurement of two-dimensional saturation fields in thin-slab systems. Water Resour. Res. 30: 2873-82.

Tu, S-C., and H. I. X. Mager. 1995. Biochemistry of bacterial bioluminescence. Photochem. Photobiol. 62: 615-624.

U. S. Department of Energy. 2000. The DOE complex-wide vadose zone science and technology roadmap: characterization, monitoring and simulation of subsurface contaminant fate and transport. Idaho Falls, ID: Idaho National Engineering and Environmental Laboratory. Draft for external review.

Uesugi, S. L., R. R. Yarwood, J. S. Selker, and P. J. Bottomley. 2001. Use of *lux*-gene dependent bioluminescence to non-intrusively quantify the cell

density of *Pseudomonas fluorescens* HK44 in translucent porous media systems. Manuscript in review.

Vandevivere, P. 1995. Bacterial clogging of porous media: a new modeling approach. Biofouling. 8: 281-291.

Vandevivere P. and P. Baveye. 1992a. Effect of bacterial extracellular polymers on the saturated hydraulic conductivity of sand columns. Appl. Environ. Microbio. 58: 1690-1698.

Vandevivere P. and P. Baveye. 1992b. Relationship between transport of bacteria and their clogging efficiency in sand columns. Appl. Environ. Microbio. 58: 2523-2530.

Vandevivere, P., and P. Baveye. 1992c. Saturated hydraulic conductivity reduction caused by aerobic bacteria in sand columns. Soil Sci. Soc. Am. J. 56: 1-13.

Vandevivere, P., and D. L. Kirchman. 1993. Attachment stimulates exopolysaccharide synthesis by a bacterium. Appl. Environ. Microbio. 59: 3280-3286.

Wan, J., J. L. Wilson, and T. L. Keift. 1994. Influence of the gas-water interface on transport of microorganisms through unsaturated porous media. Appl. Environ. Microbiol. 60: 509-516.

Webb, O. F., P. R. Bienkowski, U. Matrubutham, F. A. Evans, A. Heitzer, and G. S. Sayler. 1997. Kinetics and response of a *Pseudomonas fluorescens* HK44 biosensor. Biotechnol. Bioeng. 54: 491-502.

Wilson, T., and J. W. Hastings. 1998. Bioluminescence. Ann. Rev. Cell Devel. Biol. 14: 197-230.

Wu, J., S. Gui, P. Stahl, and R. Zhang. 1997. Experimental study on the reduction of soil hydraulic conductivity by enhanced biomass growth. Soil Sci. 162: 741-748.

Yen, K.-M., and I. C. Gunsalas. 1985. Regulation of naphthalene catabolic genes of plasmid NAH7. J. Bacteriol. 162:1008-1013.

Yen, K.-M., and C. M. Serdar. 1988. Genetics of naphthalene catabolism in pseudomonads. Crit. Rev. Microbiol. 15: 247-268.

Yeomans, C. V., F. Porteous, E. Paterson, A. A. Meharg, and K. Killham. 1999. Assessment of *lux*-marked *Pseudomonas fluorescens* for reporting on organic compounds. FEMS Microbiol. Lett. 176: 790-83.

Yolcubal, I., J. J. Pratt, S. A. Pierce, M. L. Brusseau, and R. M. Maier. 2000. Fiber optic detection of in situ *lux* reporter gene activity in porous media: system design and performance. Anal. Chem. Acta 422: 121-130.